chemistry

MDPI

Article

New Derivatives of Oleanolic Acid: Semi-Synthesis and Evaluation of Their Anti-15-LOX, Anti-α-Glucosidase and Anticancer Activities and Molecular Docking Studies

Nahla Triaa [1,2], Salma Jlizi [1], Mansour Znati [1], Hichem Ben Jannet [1] and Jalloul Bouajila [2,*]

[1] Medicinal Chemistry and Natural Products Team, Laboratory of Heterocyclic Chemistry, Natural Products and Reactivity (LR11ES39), Faculty of Science of Monastir, University of Monastir, Avenue of Environment, Monastir 5019, Tunisia; triaanahla19@gmail.com (N.T.); salma.jlizi@gmail.com (S.J.); znatimansour@yahoo.fr (M.Z.); hichem.bjannet@gmail.com (H.B.J.)

[2] Laboratoire de Génie Chimique, Université de Toulouse, CNRS, INPT, UT, 31062 Toulouse, France

* Correspondence: jalloul.bouajila@univ-tlse3.fr

Abstract: A novel series of oleanolic acid (**OA**, **1**) derivatives incorporating phenolic and coumarin moieties were synthesized. This acid was extracted from olive pomace (*Olea europaea* L.) using an ultrasound-assisted method. The structures of these novel derivatives of **OA** were characterized through the utilization of ^{1}H-NMR, ^{13}C-NMR and ESI-HRMS analyses. An evaluation of some biological activities of the prepared derivatives was conducted. The evaluation focused principally on the capacity of these structures to inhibit 15-lipoxygenase and α-glucosidase, as well as their anticancer properties when tested against tumour cell lines (HCT-116 and LS-174T) and a non-tumour cell line (HEK-293). In terms of their cytotoxic activity, the majority of the compounds exhibited notable inhibitory effects compared to the starting molecule, **OA**. Derivatives **4d**, **4k** and **4m** exhibited particularly strong inhibitory effects against the HCT-116 cell line, with IC_{50} values of 38.5, 39.3, 40.0 μM, respectively. Derivatives **4l**, **4e** and **5d** demonstrated the most effective inhibition against the LS-174T cell line, with IC_{50} values of 44.0, 44.3, 38.0 μM, respectively. However, compound **2a** was the most effective, exhibiting the most potent inhibition of 15-lipoxygenase and α-glucosidase, with IC_{50} values of 52.4 and 59.5 μM, respectively. Furthermore, molecular docking studies supported in vitro cytotoxic activity, revealing that the most potent compounds exhibited low binding energies and interacted effectively within the EGFR enzyme's active pocket (PDB: 1M17). These findings highlight the potential of these derivatives as anticancer agents and enzymatic inhibitors, warranting further investigation.

Keywords: olive pomace; oleanolic acid; coumarin; phenolics; biological activities; docking studies

check for updates

Academic Editor: George O'Doherty

Received: 12 January 2025
Revised: 28 February 2025
Accepted: 4 March 2025
Published: 7 March 2025

Citation: Triaa, N.; Jlizi, S.; Znati, M.; Ben Jannet, H.; Bouajila, J. New Derivatives of Oleanolic Acid: Semi-Synthesis and Evaluation of Their Anti-15-LOX, Anti-α-Glucosidase and Anticancer Activities and Molecular Docking Studies. *Chemistry* **2025**, *7*, 36. https://doi.org/10.3390/chemistry7020036

Copyright: © 2025 by the authors. Licensee MDPI, Basel, Switzerland. This article is an open access article distributed under the terms and conditions of the Creative Commons Attribution (CC BY) license (https://creativecommons.org/licenses/by/4.0/).

1. Introduction

The increasing prevalence of chronic and inflammatory diseases over recent decades represents a significant challenge for global public health. These chronic diseases have become a pervasive aspect of daily life, accounting for the majority of deaths globally. Despite the absence of contagion, the gradual progression and prolonged duration of these diseases have a deleterious impact on human health, accounting for 74% of global mortality [1]. Furthermore, these diseases impose a considerable financial burden on healthcare systems [2], necessitating the development of new therapeutic approaches. In this context, the significance of plants to humanity is considerable, as they provide natural solutions

for the prevention and treatment of numerous diseases, due to their abundance of bioactive compounds [3]. Moreover, 70% of the active substances utilized in pharmaceuticals originate from natural sources [4]. Among these compounds, triterpenoids, which are among the most important secondary plant metabolites, occupy a special place due to their wide variety of biological activities [5]. They are classified as terpenoids, which are also referred to as isoprenoids and terpenes. These represent the most abundant secondary metabolite class in plants. The diversity and importance of triterpenoids is demonstrated by the fact that more than 20,000 different structures have been identified, which represent a significant contribution to the field of natural product chemistry [6]. Oleanolic acid **OA** (**1**) (3β-hydroxyolea-12-en-28-oic acid) (Figure 1) has been classified within the pentacyclic triterpenoid group. Its first identification occurred in the 1970s [7]. It is present in nearly 200 species and is widely distributed in the fruits, orchards, stems and trunks of numerous edible and therapeutic plants [8,9], including *Corni fructus*, *Aralia elata* and certain medicinal herbs [7]. **OA** (**1**) is well known as an essential compound of the olive tree (*Olea europaea* L.) belonging to the Oleaceae family [10]. This compound has been demonstrated to possess a diverse range of pharmacological effects [11], including anti-inflammatory, antioxidant and anticancer properties [12]. For instance, **OA** (**1**) has been demonstrated to inhibit pro-inflammatory mediators such as TNF-α and IL-6, which enhance endogenous antioxidant defences, and induce apoptosis in cancer cells via caspase-dependent pathways. In addition to these effects, **OA** (**1**) has been shown to exert hepatoprotective effect by protecting the liver against oxidative damage and also antimicrobial properties [13]. Consequently, **OA** (**1**) has garnered significant attention in the medical and pharmaceutical research domains, given its extensive pharmacological activities [14]. On the other hand, polyphenols are bioactive compounds that are found in a wide variety of plants, including vegetables, fruit and flowers [15], and dark chocolate [16]. They are especially valued for their potent antioxidant capabilities [17]. In recent years, polyphenols have been the subject of numerous studies as potential agents for reducing the risk factors of various diseases, in particular cardiovascular disease, cancer and diabetes [18]. Moreover, coumarins, represent a notable category of natural chemical substances, given their extensive utilization in a multitude of pharmaceutical products. Some of these substances were initially isolated by Vogel in 1820 and are renowned for their anticoagulant, anti-inflammatory and antimicrobial properties [19]. Additionally, these compounds have been identified as having promising anticancer activity, including the treatment of ovarian, breast, colon, and pancreatic cancers [20]. In a recent study, Haiwei et al. [21] suggest that oleanolic acid–polyphenol derivatives exhibit anti-influenza activity. Furthermore, our research has demonstrated that the structural modification of **OA** (**1**) at the carboxyl group (C-28) is associated with enhanced anticancer activity. Furthermore, it has been demonstrated that some **OA** derivatives manifest a variety of significant biological properties [7]. The study by Vega-Granados et al. [22] indicates that the incorporation of coumarin at the C-28 position of maslinic acid, a natural structure analogous of **OA**, induces an anticancer potential against certain tumour cell lines, including Hep G2, HT29, and B16-F10.

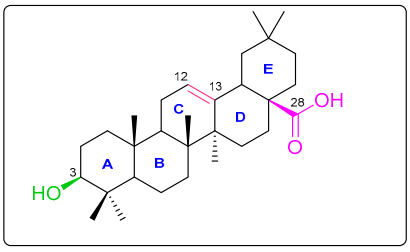

Figure 1. Oleanolic acid (**OA**, **1**).

In light of the data available in the literature, we were encouraged to synthesize **OA** derivatives by incorporating fragments of polyphenols and coumarins, with the objective of developing a more efficacious therapeutic treatment. This report details the synthesis of a series of new **OA** derivatives and provides an evaluation of their potentialanti-15-Lipoxygenase, anti-α-glucosidase and anticancer properties. In recent years, the epidermal growth factor Receptor (EGFR), a receptor tyrosine kinase, has gained prominence as a key target in cancer therapy due to its critical role in tumorigenesis and progression, particularly in colorectal cancer [23]. EGFR is over-expressed in several malignancies, including colorectal cancer [24], and its aberrant activation has been strongly linked to tumour growth, metastasis, and resistance to chemotherapy [23]. Furthermore, studies have demonstrated that colorectal cancer cell lines, such as HCT116 and LS174T, exhibit high levels of EGFR expression, making them valuable models for evaluating EGFR-targeted therapies [25–27].

Based on these considerations, EGFR was selected as the molecular target for this study. Using its crystal structure (PDB: 1M17), molecular docking simulations were performed to evaluate the binding interactions of the synthesized OA derivatives and confirm their structure-activity relationships (SAR), thereby providing insights into their potential as anticancer agents.

2. Materials and Methods

2.1. General Experimental Methods

Reagents used for part of the synthesis, media and other components used for cell culture, and reagents used for other biological activities were purchased from Sigma-Aldrich (Issy-les-Moulineaux, France). All solvents employed for synthesis and purification are of technical grade and are distilled before application. IR spectra were recorded on a FT-IR spectrometer (PerkinElmer, Waltham, MA, USA) in transmittance mode, from 4000 to 400 cm^{-1} (mid-infrared region). All new molecules were analyzed by ^{1}H-NMR, ^{13}C-NMR and HRMS. The ^{1}H-NMR spectra were obtained at frequencies of 300, 500 and 600 MHz, while the ^{13}C-NMR spectra were observed at 75, 125 and 150 MHz. Deuterated solvents, including dimethylsulfoxide-d_6 and deuterated chloroform, were employed in these experiments. All chemical shifts (δ) are expressed in ppm and are referenced to residual non-deuterated solvent. The coupling constants (*J*) are expressed in Hz. High-resolution mass spectrometry (ESI-HRMS) was performed on an Orbitrap Exactive LC-HRMS at the LCMS Competence Centre (LGC UMR 5503, Toulouse, France). Mass spectra were recorded in positive ionization mode, covering an m/z range from 70 to 1200. The temperature of the ionization source was set at 350 °C with a nebulized gas flow rate of 1.5 L/min and a dry gas flow rate of 12 L/min.

*2.2. Extraction and Isolation **OA** (**1**)*

Raw material pomace olives were procured from a factory in Sousse, Tunisia, and subsequently preserved in well-controlled conditions, devoid of light. The maceration method entailed the utilization of 3 kg of olive pomace, a solid waste product derived from the pressing of olive fruit. The pomace was subjected to an overnight drying process at 35 °C in an electric oven. Thereafter, it was immersed in 2 L of methanol at a temperature of approximately 25 °C for five days. The solution was then filtered and concentrated using a rotary evaporator to yield 43 g of extract. The extract was then treated with hexane using ultrasound, with the objective of elimination of apolar compounds such as triglycerides. The process yielded three distinct fractions: the hexane extract, a white precipitate, and an oily fraction, which were separated. The white precipitate was treated with diethyl ether, with the objective of removing more triglycerides. This process resulted in the recovery

of 30 g of a mixture of **OA** (**1**) and its analogue maslinic acid. Subsequent purification by flash chromatography was then utilized to isolate **OA** (**1**), with a total mass of 10.2 g (0.3% yield, *w*/*w*).

OA (**1**) white powder, yield 0.3%, mp: 307–311 °C (petroleum ether/EtOAc). ^{1}H-NMR (500 MHz, DMSO-d_6) δ_H 5.17 (1H, t, *J* = 3.0 Hz, H-12), 3.00 (1H, dd, *J* = 9.9; 4.7 Hz, H-3), 2.75 (1H, dd, *J* = 13.9; 4.4 Hz, H-18), 1.09 (3H, s, CH_3-27), 0.90 (3H, s, CH_3-30, 29), 0.88 (6H, s, CH_3-25), 0.85 (3H, s, CH_3-23), 0.72 (3H, s, CH_3-24), 0.68 (3H, s, CH_3-26). ^{13}C-NMR (125 MHz, DMSO-d_6) δ_C 179.06 (C-28), 144.31 (C-13), 121.98 (C-12), 77.28 (C-3), 55.26 (C-5), 47.55 (C-9), 46.15 (C-19), 45.92 (C-8 and C-17), 41.79 (C-14), 41.27 (C-18), 38.85 (C-4), 38.52 (C-1), 37.07 (C-10), 33.78 (C-21), 33.30 (C-29), 32.88 (C-7), 32.56 (C-22), 30.87 (C-20), 28.70 (C-23), 27.67 (C-2), 27.42 (C-15), 26.07 (C-27), 23.84 (C-30), 23.37 (C-11), 23.08 (C-16), 18.49 (C-6), 17.32 (C-26), 16.50 (C-24), 15.57 (C-25).

2.3. Synthesis

2.3.1. Synthesis of Compounds **2**, **2a**, **3** and **3a**

Firstly, 500 mg of the starting material **OA** (**1**) was dissolved in DMF in a round-bottomed flask with a magnetic stirrer, in the presence of (10 eq) 1,2-dibromoethane/1,3-dibromopropane and (1 eq) of potassium carbonate (K_2CO_3). The reaction mixture is then kept at ambient temperature during 16 h. Next, 100 mL of distilled water was added to the resulting organic solution and then extracted with ethyl acetate. The organic layer was subjected to drying over sodium sulphate, filtration, and solvent evaporation to give a dry residue that was purified through a silica gel column chromatography eluted with petroleum ether/ethyl acetate (8:2, *v*/*v*). Four products (**2**, **2a**, **3** and **3a**) were obtained, with yields of 69, 8, 71 and 9%, respectively.

2-Bromoethyl (4aS,6aS,6bR,8aR,10S,12aR,12bR,14bS)-10-hydroxy-2,2,6a,6b,9,9,12a-heptamethyl-1,3,4,5,6,6a,6b,7,8,8a,9,10,11,12,12a,12b,13,14b-octadecahydropicene-4a(2H)-carboxylate (**2**)

White solid; Rf = 0.65 (cyclohexane/EtOAc, 70:30), yield 69%, 345 mg, mp: 166–169 °C (EtOAc). IR (ν_{max}/cm^{-1}) 3395.07 (OH), 2931.32 (CH str.), 1727.22 (C=O), 657.28 (C-Br). ^{1}H-NMR (500 MHz, $CDCl_3$) δ_H 5.33 (1H, t, *J* = 3.5 Hz, H-12), 4.35 (2H, m, H-1′), 3.52 (2H, t, *J* = 5.9 Hz, H-2′), 3.23 (1H, dd, *J* = 11.1; 4.1 Hz, H-3), 2.90 (1H, dd, *J* = 13.7; 4.3 Hz, H-18), 1.15 (3H, s), 1.00 (3H, s), 0.95 (3H, s), 0.92 (6H, s), 0.79 (3H, s), 0.75 (3H, s). ^{13}C-NMR (125 MHz, $CDCl_3$) δ_C 177.33, 143.49, 122.64, 79.02, 63.63 (C-1′), 55.22, 47.61, 46.87, 45.81, 41.70, 41.28, 39.38, 38.76, 38.46, 37.03, 33.85, 33.09, 32.74, 32.45, 30.70, 29.08 (C-2′), 28.11, 27.70, 27.20, 25.86, 23.60, 23.43, 22.95, 18.34, 17.05, 15.59, 15.33. ESI-HRMS calculated for $C_{32}H_{51}BrO_3Na$ [M + Na]$^+$: 585.2919, found: 585.2915. Δm = −0.68 ppm.

(4aS,4a′S,6aS,6bR,6a′S,6b′R,8aR,8a′R,10S,10′S,12aR,12bR,12a′R,12b′R,14bS,14b′S)-Bis(10-hydroxy-2,2,6a,6b,9,9,12a-heptamethyl-1,3,4,5,6,6a,6b,7,8,8a,9,10,11,12,12a,12b,13,14b-octadecahydropicene-4a(2H)-carboxylate) (**2a**)

White solid; Rf = 0.55 (cyclohexane/EtOAc, 60:40), yield 8%, 40 mg, mp: 175–177 °C (EtOAc). IR (ν_{max}/cm^{-1}) 3380.30 (2 × OH), 2926.40 (CH str.), 1722.29 (2 × C=O). ^{1}H-NMR (500 MHz, $CDCl_3$) δ_H 5.32 (2H, m, H-12 × 2), 4.20 (4H, m, H-1′ × 2), 3.81 (4H, s, H-2′ × 2), 3.23 (2H, d, *J* = 3.23 Hz, H-3 × 2), 2.88 (2H, d, *J* = 13.40 Hz, H-18 × 2), 1.16 (6H, s), 1.00 (6H, s), 0.95 (6H, s), 0.92 (12H, s), 0.80 (6H, s), 0.76 (6H, s). ^{13}C-NMR (125 MHz, $CDCl_3$) δ_C 178.17, 177.48, 144.58, 144.14, 122.53, 122.35, 79.01, 66.07 (C-1′,2′), 62.20, 61.47, 55.20, 55.20, 47.61, 46.94, 46.71, 45.83, 45.79, 41.80, 41.71, 41.49, 41.28, 39.34, 39.33, 38.75, 38.45, 37.05, 37.02, 33.86, 33.82, 33.08, 32.72, 32.49, 32.43, 30.71,30.69, 28.11, 27.79, 27.64, 27.18, 25.89, 25.86, 23.63, 23.42, 23.05, 18.33, 18.31, 17.03, 16.93, 15.58, 15.34, 15.32. ESI-HRMS calculated for $C_{62}H_{98}O_6Na$ [M + Na]$^+$: 961.7261, found: 961.7245. Δm = −1.66 ppm.

3-Bromopropyl (4aS,6aS,6bR,8aR,10S,12aR,12bR,14bS)-10-hydroxy-2,2,6a,6b,9,9,12a-heptamethyl-1,3,4,5,6,6a,6b,7,8,8a,9,10,11,12,12a,12b,13,14b-octadecahydropicene-4a(2H)-carboxylate (**3**)

White solid; Rf = 0.66 (cyclohexane/EtOAc, 70:30), yield 71%, 355 mg, mp: 160–165 °C (EtOAc). IR (ν_{max}/cm^{-1}) 3413.95 (OH), 2926.40 (CH str.), 1727.22 (C=O), 656.90 (C-Br). ^{1}H-NMR (600 MHz, $CDCl_3$) δ_H 5.30 (1H, t, *J* =3.6 Hz, H-12), 4.35 (2H, m, H-1′), 3.49 (2H, t, *J* = 6.5 Hz, H-3′), 3.23 (1H, dd, *J* = 11.2; 4.2 Hz, H-3), 2.87 (1H, dd, *J* = 13.8; 4.3 Hz, H-18), 1.15 (3H, s), 1.00 (3H, s), 0.94 (3H, s), 0.92 (3H, s), 0.92 (3H, s), 0.79 (3H, s), 0.76 (3H, s). ^{13}C-NMR (150 MHz, $CDCl_3$) δ_C 177.53, 143.76, 122.52, 79.02, 61.82 (C-1′), 55.22, 47.62, 46.83, 45.81, 41.74, 41.40, 39.34, 38.76, 38.45, 37.04, 33.84, 33.10, 32.74, 32.50, 31.78, 30.71, 29.60, 28.12, 27.65, 27.20, 25.89, 23.63, 23.46, 23.04, 18.34, 17.14, 15.58, 15.32. ESI-HRMS calculated for $C_{33}H_{53}BrO_3Na$ $[M + Na]^+$: 599.3076, found: 599.3069. Δm = −1.16 ppm.

Propane-1,3-diyl(4aS,4a′S,6aS,6bR,6a′S,6b′R,8aR,8a′R,10S,10′S,12aR,12bR,12a′R,12b′R,14bS,14b′S)-bis(10-hydroxy-2,2,6a,6b,9,9,12a-heptamethyl-1,3,4,5,6,6a,6b,7,8,8a,9,10,11,12,12a,12b,13,14b-octadecahydropicene-4a(2H)-carboxylate) (**3a**)

White solid; Rf = 0.58 (cyclohexane/EtOAc, 60:40), yield 9%, 45 mg, mp: 185–188 °C (EtOAc). ^{1}H-NMR (600 MHz, $CDCl_3$) δ_H 5.22 (2H, t, *J* = 3.5 Hz, H-12 × 2), 4.02 (4H, t, *J* = 6.3 Hz, H-1′,3′), 3.14 (2H, dd, *J* = 11.2; 4.2 Hz, H-3 × 2), 2.78 (2H, dd, *J* = 13.8; 4.2 Hz, H-18 × 2), 1.16 (6H, s), 0.91 (6H, s), 0.85 (6H, s), 0.83 (12H, s), 0.70 (6H, s), 0.65 (6H, s). ^{13}C-NMR (150 MHz, $CDCl_3$) δ_C 177.58, 143.73, 122.46, 79.01, 60.84 (C-1′,3′), 55.19, 47.60, 46.75, 45.84, 41.72, 41.35, 39.33, 38.75, 38.44, 37.03, 33.87, 33.11, 32.76, 32.49, 30.70, 28.15, 28.11, 27.67, 27.20, 25.88, 23.65, 23.44, 23.01, 18.34, 17.08, 15.59, 15.36. ESI-HRMS calculated for $C_{63}H_{100}O_6Na$ $[M + Na]^+$: 975.7418, found: 975.7370. Δm = −4.91 ppm.

2.3.2. Synthesis of Compounds **4a**–**n** and **5a**–**f**

To 75 mg of compound **2** (or **3**) dissolved in DMF under magnetic stirring, 1 eq of polyphenol or coumarin and cesium carbonate (Cs_2CO_3) (2 eq) as a base were added. After 48h, 15 mL of distilled water was added and the resultant solution was extracted twice with ethyl acetate. The organic layer was purified by flash chromatography, employing a mixture of cyclohexane and ethyl acetate (6:4, *v*/*v*) as eluent, to afford compounds **4a**–**n** and **5a**–**f** with yields ranging from 68 to 79%, respectively (Scheme 1).

2-(4-(Methoxycarbonyl)phenoxy)ethyl(4aS,6aS,6bR,8aR,10S,12aR,12bR,14bS)-10-hydroxy-2,2,6a,6b,9,9,12a-heptamethyl-1,3,4,5,6,6a,6b,7,8,8a,9,10,11,12,12a,12b,13,14b-octadecahydropicene-4a(2H)-carboxylate (**4a**)

White solid; Rf = 0.45 (cyclohexane/EtOAc, 80:20), yield 68%, 51 mg, mp: 128–130 °C (EtOAc). IR (ν_{max}/cm^{-1}) 3347.74 (OH), 2941.17 (CH str.), 1703.41 (2 × C=O), 1603.28 (C=C Ar). ^{1}H-NMR (500 MHz, $CDCl_3$) δ_H 8.01 (2H, dd, *J* = 6.8; 2.0, H-6″, 2″), 6.93 (2H, dd, *J* = 6.8; 2.0, H-5″, 3″), 5.27 (1H, t, *J* = 3.5 Hz, H-12), 4.42 (2H, m, H-1′), 4.23 (2H, t, *J* = 4.6 Hz, H-2′), 3.91 (3H,s, H-8″),3.22 (1H, dd, *J* = 11.0; 4.2 Hz, H-3), 2.89 (1H, dd, *J* = 13.6; 4.5 Hz, H-18), 1.13 (3H, s), 0.99 (3H, s), 0.93 (3H, s), 0.91 (3H, s), 0.84 (3H, s), 0.78 (3H, s), 0.66 (3H, s). ^{13}C-NMR (125 MHz, $CDCl_3$) δ_C 177.72, 166.78 (C-4″), 162.34 (C-7″), 143.55, 131.64 (C-Ar), 122.95 (C-1″), 122.54, 114.17 (C-Ar), 79.02, 66.06 (C-2′), 62.33 (C-2′), 55.18, 51.91, 47.57, 46.83, 45.82, 41.66, 41.26, 39.30, 38.74, 38.41, 36.99, 33.82, 33.08, 32.62, 32.43, 30.69, 28.10, 27.61, 27.18, 25.86, 23.61, 23.39, 22.95, 18.26, 16.98, 15.56, 15.23. ESI-HRMS calculated for $C_{40}H_{58}O_6Na$ $[M + Na]^+$: 657.4131, found: 657.4130. Δm = −0.15 ppm.

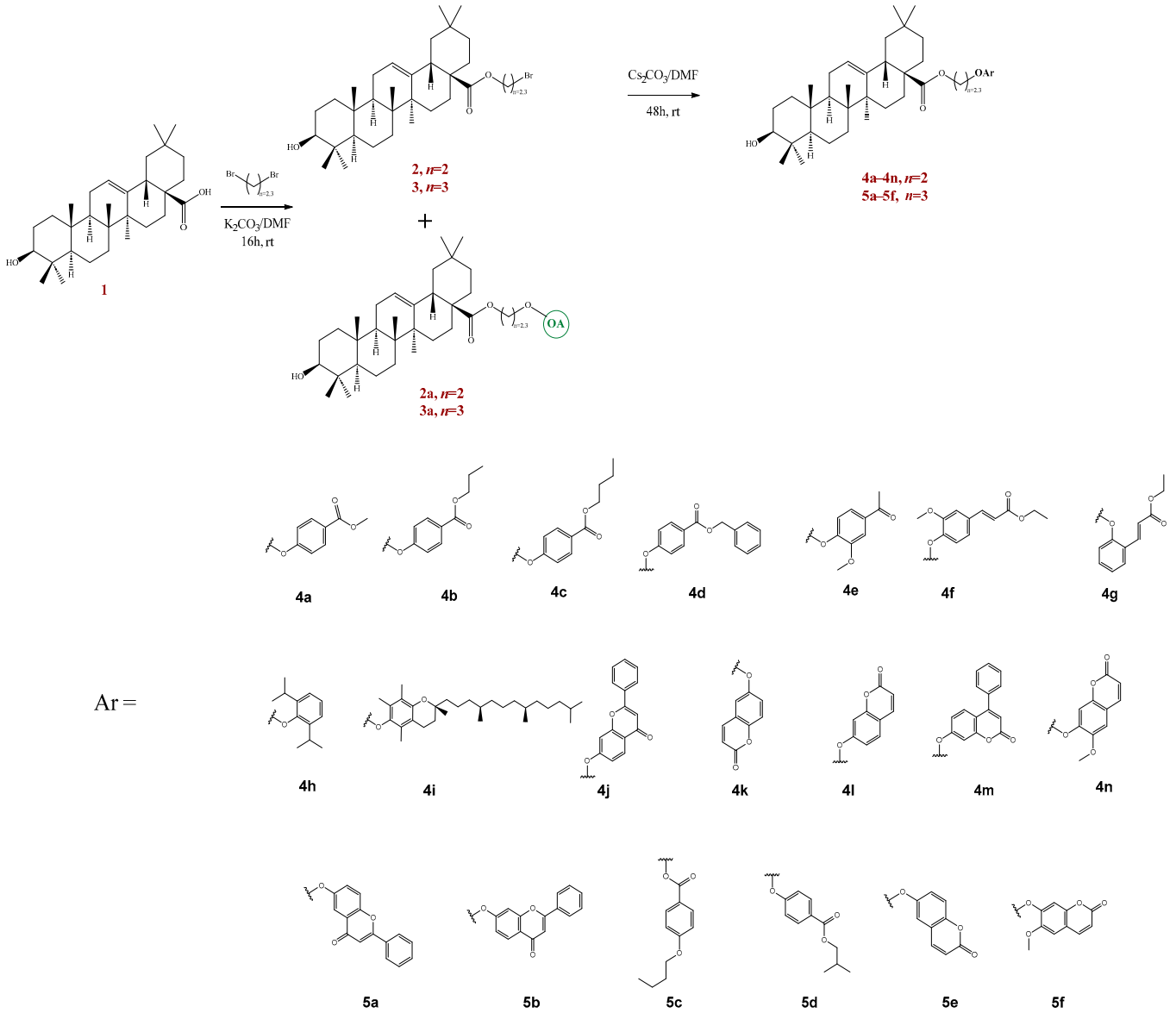

Scheme 1. Synthetic pathways of **4a–n** and **5a–f** derivatives of **OA**.

2-(4-(Propoxycarbonyl)phenoxy)ethyl(4aS,6aS,6bR,8aR,10S,12aR,12bR,14bS)-10-hydroxy-2,2,6a,6b,9,9,12a-heptamethyl-1,3,4,5,6,6a,6b,7,8,8a,9,10,11,12,12a,12b,13,14b-octadecahydropicene-4a(2H)-carboxylate (**4b**)

White solid; Rf = 0.50 (cyclohexane/EtOAc, 70:30), yield 71%, 53 mg, mp: 126–128 °C (EtOAc). IR (ν_{max}/cm^{-1}) 3547.74 (OH), 2931.32 (CH str.), 1708.34 (2 × C=O), 1608.20 (C=C Ar). ^{1}H-NMR (600 MHz, $CDCl_3$) δ_H 7.94 (2H, dd, *J* = 6.8; 2.0 Hz, H-Ar), 6.84 (2H, dd, *J* = 6.8; 2.0 Hz, H-Ar), 5.18 (1H, t, *J* = 3.6 Hz, H-12), 4.33 (2H, m, H-1′), 4.19 (2H, t, *J* = 6.6 Hz, H-2′), 4.15 (2H, t, *J* = 4.6 Hz, H-8″), 3.13 (1H, dd, *J* = 12.0; 6.0 Hz, H-3), 2.81 (1H, dd, *J* = 13.8; 4.3 Hz, H-18), 1.05 (3H, s), 0.96 (3H, t, *J* = 7.4 Hz, H-10″), 0.91 (3H, s), 0.84 (3H, s), 0.82 (3H, s), 0.75 (3H, s), 0.69 (3H, s), 0.57 (3H, s). ^{13}C-NMR (150 MHz, $CDCl_3$) δ_C 177.72, 166.36 (C-4″), 162.26 (C-7″), 143.55, 131.58 (C-Ar), 123.32 (C-1″), 122.55, 114.13 (C-Ar), 79.02, 66.29 (C-8″), 66.06 (C-2′), 62.33 (C-1′), 55.18, 47.57,46.83, 45.82, 41.66, 41.27, 39.30, 38.73, 38.41, 36.98, 33.82, 33.08, 32.62, 32.43, 30.69, 28.09, 27.60, 27.18, 25.86, 23.62, 23.38, 22.95, 22.18, 18.26, 16.98, 15.55, 15.23, 10.55. ESI-HRMS calculated for $C_{42}H_{62}O_6Na$ $[M + Na]^+$: 685.4444, found: 685.4437. Δm = −1.02 ppm.

2-(4-(Butoxycarbonyl)phenoxy)ethyl(4aS,6aS,6bR,8aR,10S,12aR,12bR,14bS)-10-hydroxy-2,2,6a,6b,9,9,12a-heptamethyl-1,3,4,5,6,6a,6b,7,8,8a,9,10,11,12,12a,12b,13,14b-octadecahydropicene-4a(2H)-carboxylate (**4c**)

White solid; Rf = 0.57 (cyclohexane/EtOAc, 70:30), yield 69%, 52 mg, mp: 110–115 °C (cyclohexane/EtOAc). IR (ν_{max}/cm^{-1}) 3332.69 (OH), 2931.32 (CH str.), 1713.26 (2 × C=O), 1598.35 (C=C Ar). ^{1}H-NMR (600 MHz, $CDCl_3$) δ_H 7.93 (2H, dd, *J* = 6.9; 2.0 Hz, H-Ar), 6.84 (2H, dd, *J* = 6.9, 2.0 Hz, H-4″), 5.18 (1H, t, *J* = 3.5 Hz, H-12), 4.33 (2H, m, H-1′), 4.23 (2H, t, *J* = 6.6 Hz, H-2′), 4.15 (2H, dd, *J* = 10.1; 4.6 Hz, H-8″), 3.13 (1H, m, H-3), 2.80 (1H,dd, *J* = 13.8; 4.1 Hz, H-18), 1.04 (3H, s), 0.91 (6H, s), 0.84 (3H, s),0.82 (3H,s),0.75 (3H, s), 0.69 (3H, s), 0.57 (3H, s). ^{13}C-NMR (150 MHz, $CDCl_3$) δ_C 177.72, 166.37 (C-4″), 162.25 (C-7″), 143.54, 131.57 (C-Ar), 123.32 (C-1″), 122.55, 114.13 (C-Ar), 79.01, 66.06 (C-2′), 64.60 (C-8″), 62.33 (C-1′), 55.20, 47.57, 46.83, 45.82, 41.66, 41.26, 39.30, 38.73, 38.41, 36.98, 33.82, 33.08, 32.62, 32.43, 30.85, 30.69, 28.10, 27.60, 27.18, 25.86, 23.62, 23.38, 22.95, 19.30, 18.26, 16.98, 15.56, 15.23, 13.80. ESI-HRMS calculated for $C_{43}H_{64}O_6Na$ $[M + Na]^+$: 699.4601, found: 699.4588. Δm = −1.85 ppm.

2-(4-((Benzyloxy)carbonyl)phenoxy)ethyl(4aS,6aS,6bR,8aR,10S,12aR,12bR,14bS)-10-hdroxy-2,2,6a,6b,9,9,12a-heptamethyl-1,3,4,5,6,6a,6b,7,8,8a,9,10,11,12,12a,12b,13,14b-octadecahydropicene-4a(2H)-carboxylate (**4d**)

White solid; Rf = 0.50 (cyclohexane/EtOAc, 80:20), yield 77%, 58 mg, mp: 142–145 °C (EtOAc). IR (ν_{max}/cm^{-1}) 3547.74 (OH), 2926.40 (CH str.), 1716.55 (2 × C=O), 1598.35 (C=C Ar). ^{1}H-NMR (500 MHz, $CDCl_3$) δ_H 8.06 (2H, dd, *J* = 6.9; 2.0 Hz, H-6″, 2″), 7.40 (5H, m, H-Ar), 5.36 (2H, s, H-8″), 5.26 (1H, t, *J* = 3.5 Hz, H-12), 4.41 (2H, m, H-1′), 4.24 (2H, t, *J* = 4.6 Hz, H-2′), 3.22 (1H, dd, *J* = 11.1; 4.0 Hz, H-3), 2.89 (1H, dd, *J* = 13.8; 4.4 Hz, H-18), 1.13 (3H, s), 0.99 (3H, s), 0.93 (3H, s), 0.91 (3H, s), 0.84 (3H, s), 0.78 (3H, s), 0.66 (3H, s). ^{13}C-NMR (125 MHz, $CDCl_3$) δ_C 177.72, 166.11 (C-4″), 162.46 (C-7″), 143.54, 136.26 (C-9″), 131.91 (C-Ar), 128.60 (C-Ar), 128.17 (C-Ar), 128.11 (C-Ar), 122.89 (C-1″), 122.55, 114.19 (C-Ar), 79.02, 66.43 (C-2′), 66.07 (C-8″), 62.32 (C-1′), 55.18, 47.57, 46.83, 45.82, 41.66, 41.27, 39.31, 38.74, 38.42, 36.98, 33.82, 33.08, 32.63, 32.43, 30.69, 28.11, 27.60, 27.19, 25.86, 23.62, 23.39, 22.95, 18.17, 16.98, 15.58, 15.24. ESI-HRMS calculated for $C_{46}H_{62}O_6Na$ $[M + Na]^+$: 733.4444, found: 733.4445. Δm = 0.13 ppm.

2-(4-Acetyl-2-methoxyphenoxy)ethyl(4aS,6aS,6bR,8aR,10S,12aR,12bR,14bS)-10-hydroxy-2,2,6a,6b,9,9,12a-heptamethyl-1,3,4,5,6,6a,6b,7,8,8a,9,10,11,12,12a,12b,13,14b-octadecahydropicene-4a(2H)-carboxylate (**4e**)

White solid; Rf = 0.33 (cyclohexane/EtOAc, 70:30), yield 73%, 55.75 mg, mp: 148–150 °C (EtOAc). IR (ν_{max}/cm^{-1}) 3547.74 (OH), 2917.37 (CH str.), 1728.04 (C=O), 1674.69 (C=O), 1588.50 (C=C Ar). ^{1}H-NMR (600 MHz, $CDCl_3$) δ_H 7.49 (1H, dd, *J* = 1.8; 8.4 Hz, H-6″), 7.47 (1H, d, *J* = 1.8 Hz, H-2″), 6.83 (1H, d, *J* = 8.4 Hz, H-5″), 5.14 (1H, t, *J* = 3.6 Hz, H-12), 4.38 (2H, m, H-1′), 4.23 (2H, t, *J* = 5.0 Hz, H-2′), 3.85 (3H, s, H-9″), 3.12 (1H, dd, *J* = 11.4; 4.8 Hz, H-3). 2.79 (1H, dd, *J* = 13.8; 4.2 Hz, H-18), 2.51 (3H, s, H-8″), 1.02 (3H, s), 0.89 (3H, s), 0.83 (3H, s), 0.81 (3H, s), 0.71 (3H, s), 0.67 (3H, s), 0.50 (3H, s). ^{13}C-NMR (150 MHz, $CDCl_3$) δ_C 196.97 (C-7″), 177.82, 152.32 (C-4″), 149.32 (C-3″), 143.51, 130.75 (C-1″), 123.17, 122.40 (C-6″), 111.55 (C-5″), 110.34 (C-10), 78.98, 66.44 (C-2′), 61.85 (C-2′), 55.98, 55.05, 47.46, 46.78, 45.74, 41.58, 41.18, 39.18, 38.72, 38.33, 36.92, 33.78, 33.14, 32.48, 32.35, 30.73, 28.09, 27.54, 27.12, 26.38, 25.89, 23.65, 22.32, 22.87, 18.26, 16.88, 15.60, 15.22. ESI-HRMS calculated for $C_{41}H_{60}O_6Na$ $[M + Na]^+$: 671.4288, found: 671.4273. Δm = −2.23 ppm.

2-(4-((E)-3-Ethoxy-3-oxoprop-1-en-1-yl)-2-methoxyphenoxy)ethyl(4aS,6aS,6bR,8aR,10S,12aR,12bR,14bS)-10-hydroxy-2,2,6a,6b,9,9,12a-heptamethyl-1,3,4,5,6,6a,6b,7,8,8a,9,10,11,12,12a,12b,13,14b-octadecahydropicene-4a(2H)-carboxylate (**4f**)

White solid; Rf = 0.39 (cyclohexane/EtOAc, 70:30), yield 69%, 51.75 mg, mp: 135–139 °C (EtOAc). ^{1}H-NMR (300 MHz, $CDCl_3$) δ_H 7.64 (1H, d, *J* = 15.9 Hz, H-3″),

7.09 (2H,m, H-Ar), 6.90 (1H, d, *J* = 8.1 Hz, H-5″), 6.33 (1H, d, *J* = 15.9 Hz, H-2″), 5.25 (1H, t, *J* = 3.3 Hz, H-12), 4.41 (2H, m, H-1′), 4.31 (2H, m, H-2′), 4.26 (2H, m, H-10″), 3.90 (3H, s, H-12″), 3.22 (1H, dd, *J* = 10.3; 5.3 Hz, H-3), 2.89 (1H, dd, *J* = 12.0; 3.0 Hz, H-18), 1.36 (3H, t, *J* = 7.1 Hz, H-11″), 1.13 (3H, s), 1.00 (3H, s), 0.93 (3H, s), 0.91 (3H, s), 0.86 (3H, s), 0.78 (3H, s), 0.65 (3H, s). ^{13}C-NMR (150 MHz, $CDCl_3$) δ_C177.70, 167.04 (C-1″), 144.52 (C-7″), 143.18 (C-6″), 137.98 (C-3″), 127.94, 122.53 (C-4″), 122.33, 117.49 (C-9″), 116.26 (C-8″), 113.39 (C-2″), 110.35 (C-5″), 79.01, 66.98 (C-2′), 62.34 (C-1′), 60.43 (C-10″), 55.92 (C-12), 55.14, 50.92, 47.54, 46.78, 45.82, 41.63, 41.24, 39.24, 38.24, 38.41, 36.97, 33.84, 32.57, 32.37, 30.69, 28.07, 27.62, 27.17, 25.86, 24.81, 23.61, 22.92, 16.87, 16.37, 15.56, 1524, 14.36. ESI-HRMS calculated for $C_{44}H_{64}O_7Na$ $[M + Na]^+$: 727.4550, found: 727.4547. Δm = −0.41 ppm.

2-(2-((E)-3-Ethoxy-3-oxoprop-1-en-1-yl)phenoxy)ethyl(4aS,6aS,6bR,8aR,10S,12aR,12bR, 14bS)-10-hydroxy-2,2,6a,6b,9,9,12a-heptamethyl-1,3,4,5,6,6a,6b,7,8,8a,9,10,11,12,12a,12b,13, 14b-octadecahydropicene-4a(2H)-carboxylate (**4g**)

White solid; Rf = 0.45 (cyclohexane/EtOAc, 70:30), yield 68%, 51 mg, mp: 134–138 °C (acetonitrile). IR (ν_{max}/cm^{-1}) 3313.81 (OH), 2936.25 (CH str.), 1713.26 (2 × C=O), 1632.01 (C=C Ar). ^{1}H-NMR (300 MHz, $CDCl_3$) δ_H 7.95 (1H, d, *J* = 16.1 Hz, H-3″), 7.49 (1H, dd, *J* = 7.7; 1.5 Hz, H-9″), 7.31 (1H, m, H-Ar), 6.92 (1H, m, H-Ar), 6.56 (1H, d, *J* = 16.1 Hz, H-2″), 5.21 (1H, t, *J* = 3.5 Hz, H-12), 4.45 (2H, m, H-1′), 4.21 (4H, m, H-2′, 10″), 3.18 (1H, dd, *J* = 10.5; 5.7 Hz, H-3), 2.87 (1H, dd, *J* = 13.6; 4.3 Hz, H-18), 1.08 (3H, s), 0.96 (3H, s), 0.89 (3H, s), 0.87 (3H, s), 0.79 (3H, s), 0.75 (3H, s), 0.58 (3H, s). ^{13}C-NMR (75 MHz, $CDCl_3$) δ_C 177.67, 167.33 (C-1″), 157.36 (C-5″), 143.54, 139.88 (C-3″), 131.18 (C-9″), 129.37 (C-7″), 123.89 (C-4″), 122.57, 121.11 (C-8″), 119.32 (C-2″), 112.19 (C-6″), 79.01, 66.50 (C-2′), 62.37 (C-1′), 60.19, 55.25, 47.62, 46.88, 45.91, 41.70, 41.33, 39.34, 38.72, 38.47, 37.01, 33.88, 33.02, 32.64, 32.45, 30.62, 28.09, 27.70, 27.22, 25.80, 23.57, 23.33, 22.97, 18.26, 16.93, 15.50, 15.16, 14.34. ESI-HRMS calculated for $C_{43}H_{62}O_6Na$ $[M + Na]^+$: 697.4444, found: 697.4443. Δm = −0.14 ppm.

2-(2,6-Diisopropylphenoxy)ethyl(4aS,6aS,6bR,8aR,10S,12aR,12bR,14bS)-10-hydroxy-2,2,6a,6b,9,9,12a-heptamethyl-1,3,4,5,6,6a,6b,7,8,8a,9,10,11,12,12a,12b,13,14b-octadecahydropicene-4a(2H)-carboxylate (**4h**)

White solid; Rf = 0.56 (cyclohexane/EtOAc, 70:30), yield 71%, 53.20 mg, mp: 142–145 °C (acetonitrile). IR (ν_{max}/cm^{-1}) 3275.23 (OH), 2941.17 (CH str.), 1728.04 (C=O). ^{1}H-NMR (300 MHz, $CDCl_3$) δ_H 7.09 (2H, s, H-Ar), 5.31 (1H, t, *J* = 3.5 Hz, H-12), 4.36 (2H, m, H-1′), 3.93 (2H, m, H-2′), 3.34 (2H, m, H-7″, 10″), 3.20 (1H, m, H-3), 2.93 (1H, dd, *J* = 15.0; 3.0 Hz, H-18), 1.22 (12H, dd, *J* = 6.9; 1.7 Hz, H-9″-12″), 1.14 (3H, s), 0.97 (3H, s), 0.95 (3H, s), 0.91 (3H, s), 0.89 (3H, s), 0.76 (3H, s), 0.75 (3H, s). ^{13}C-NMR (75 MHz, CDCl3) δ_C 177.63, 152.76 (C-1″), 143.71,141.73 (C-Ar), 124.74 (C-Ar), 124.04 (C-Ar), 122.54, 79.02, 72.15 (C-2′), 63.61 (C-1′), 55.32, 47.70, 46.79, 45.92, 41.76, 41.49, 39.42, 38.75, 38.52, 37.08, 33.94, 33.05, 32.77, 32.42, 30.68, 28.09, 27.80, 27.25, 26.37, 25.92, 24.03, 23.65, 23.43, 23.05, 18.34, 16.63, 15.50, 15.26. ESI-HRMS calculated for $C_{44}H_{68}O_4Na$ $[M + Na]^+$: 683.5015, found: 683.5008. Δm = −1.02 ppm.

2-(((R)-2,5,7,8-Tetramethyl-2-((4R,8R)-4,8,12-trimethyltridecyl)chroman-6-yl)oxy)ethyl (4aS,6aS,6bR,8aR,10S,12aR,12bR,14bS)-10-hydroxy-2,2,6a,6b,9,9,12a-heptamethyl-1,3,4,5,6, 6a,6b,7,8,8a,9,10,11,12,12a,12b,13,14b-octadecahydropicene-4a(2H)-carboxylate (**4i**)

Yellow solid; Rf = 0.42 (cyclohexane/EtOAc, 80:20), yield 77%, 57.75 mg, mp: 124–128 °C (acetonitrile). ^{1}H-NMR (300 MHz, $CDCl_3$) δ_H 5.24 (1H, t, *J* = 3.3 Hz, H-12), 4.27 (2H, m, H-1′), 3.72 (2H, m, H-2′), 3.20 (1H, dd, *J* = 10.2; 5.1 Hz, H-3), 2.88 (1H, dd, *J* = 14.1; 3.9 Hz, H-18), 2.57 (2H, t, *J* = 6.0 Hz, H-4″), 2.15 (3H, s), 2.11(3H, s), 2.01(3H, s), 1.25 (3H, s), 1.12 (3H, s), 0.98 (3H, s), 0.92(3H, s), 0.89 (3H, s), 0.87 (6H, s), 0.85 (6H, s), 0.77 (3H, s), 0.72 (3H, s). ^{13}C-NMR (75 MHz, $CDCl_3$) δ_C 177.55, 148.23 (C-6″), 147.85 (C-3″), 143.80, 127.66 (C-7″), 125.60 (C-8″), 122.67, 122.46 (C-5″), 117.51 (C-4″), 79.03, 74.76 (C-1″), 69.37 (C-2′), 61.21 (C-1′), 55.31, 47.68, 46.74, 46.00, 41.77, 41.41, 39.42, 39.38, 38.75, 38.50, 37.38, 37.07,

33.95, 33.03, 32.78, 32.70, 32.52, 31.38, 30.66, 29.70, 28.11, 27.94, 27.72, 27.26, 25.84, 24.75, 24.41, 23.81, 23.59, 23.37, 23.14, 22.63, 22.55, 21.02, 20.65, 19.70, 19.64, 18.35, 17.07, 15.21, 12.67, 11.80, 11.71. ESI-HRMS calculated for $C_{61}H_{100}O_5Na$ $[M + Na]^+$: 935.7468, found: 935.7516. Δm = 5.12 ppm.

2-((4-Oxo-2-phenyl-4H-chromen-7-yl)oxy)ethyl(4aS,6aS,6bR,8aR,10S,12aR,12bR,14bS)-10-hydroxy-2,2,6a,6b,9,9,12a-heptamethyl-1,3,4,5,6,6a,6b,7,8,8a,9,10,11,12,12a,12b,13,14b-octadecahydropicene-4a(2H)-carboxylate (**4j**)

White solid; Rf = 0.42 (cyclohexane/EtOAc, 50:50), yield 75%, 56 mg, mp: 134–138 °C (EtOAc). ^{1}H-NMR (500 MHz, $CDCl_3$) δ_H 8.18 (1H, d, *J* = 8.8 Hz, H-5″), 7.94 (2H, m, H-12″, 16″), 7.55 (3H, m, H-13″, 14″, 15″), 7.03 (1H, dd, *J* = 8.8; 2.3 Hz, H-6″), 7.00 (1H,d, *J* = 2.3 Hz, H-8″), 6.81 (1H, s, H-3″), 5.27 (1H, t, *J* = 3.5 Hz, H-12), 4.48 (2H, m, H-1′), 4.33 (2H, m, H-2′), 3.20 (1H, dd, *J* = 10.0; 5.0 Hz, H-3), 2.89 (1H, dd, *J* = 13.5; 4.5 Hz, H-18), 1.12 (3H, s), 0.95 (3H, s), 0.93 (3H, s), 0.91 (3H, s), 0.82 (3H, s), 0.71 (3H, s), 0.70 (3H, s). ^{13}C-NMR (125 MHz, $CDCl_3$) δ_C 177.82 (C-4″), 177.72, 163.14 (C-7″), 157.89 (C-2″), 143.56, 131.81 (C-9″), 131.52 (C-5″), 129.07 (C-Ar), 127.07 (C-Ar), 126.16 (C-Ar), 122.54, 118.13 (C-10″), 114.52 (C-6″), 107.56 (C-3″), 101.40 (C-8″), 78.97, 66.60 (C-2′), 62.21 (C-1′), 55.13, 47.53, 46.85, 45.82, 41.65, 41.26, 39.31, 38.69, 38.37, 36.97, 33.81, 33.05, 32.59, 32.45, 30.68, 29.71, 28.05, 27.59, 27.14, 25.84, 23.59, 23.38, 22.98, 18.23, 17.05, 15.49, 15.19. ESI-HRMS calculated for $C_{47}H_{60}O_6Na$ $[M + Na]^+$: 743.4288, found: 743.4288. Δm = 0 ppm.

2-((2-Oxo-2H-chromen-6-yl)oxy)ethyl(4aS,6aS,6bR,8aR,10S,12aR,12bR,14bS)-10-hydroxy-2,2,6a,6b,9,9,12a-heptamethyl-1,3,4,5,6,6a,6b,7,8,8a,9,10,11,12,12a,12b,13,14b-octadecahydropicene-4a(2H)-carboxylate (**4k**)

White solid; Rf = 0.46 (cyclohexane/EtOAc, 70:30), yield 79%, 59 mg, mp: 113–116 °C (acetonitrile). ^{1}H-NMR (600 MHz, $CDCl_3$) δ_H 7.58 (1H, d, *J* = 9.5 Hz, H-4″), 7.21 (1H, d, *J* = 9.0 Hz, H-8″), 7.05 (1H, dd, *J* = 9.0; 2.9 Hz, H-7″), 6.85 (1H, d, *J* = 2.9 Hz, H-5″), 6.38 (1H, d, *J* = 9.5 Hz, H-3″), 5.18 (1H, t, *J* = 3.6 Hz, H-12), 4.33 (2H, m, H-1′), 4.13 (2H, m, H-2′), 3.13 (1H, m, H-3), 2.80 (1H, m, H-18), 1.04 (3H, s), 0.91 (3H, s), 0.89 (3H, s), 0.83 (3H, s), 0.75 (3H, s), 0.69 (3H, s), 0.58 (3H, s). ^{13}C-NMR (150 MHz, $CDCl_3$) δ_C 177.71, 160.87 (C-6″), 155.11 (C-2″), 148.69 (C-9″), 143.56, 143.04 (C-4″), 122.51, 119.95 (C-8″), 119.20 (C-10″), 118.01 (C-7″), 117.26 (C-3″), 111.06 (C-5″), 78.98, 66.75 (C-2′), 62.37 (C-1′), 55.16, 47.54, 46.83, 45.81, 41.67, 41.28, 39.31, 38.74, 38.41, 36.99, 33.82, 33.07, 32.65, 32.44, 30.69, 28.09, 27.62, 27.17, 25.85, 23.61, 23.38, 22.97, 18.27, 17.02, 15.57, 15.23. ESI-HRMS calculated for $C_{41}H_{56}O_6Na$ $[M + Na]^+$: 667.3975, found: 667.3979. Δm = −0.59 ppm.

2-((2-Oxo-2H-chromen-7-yl)oxy)ethyl(4aS,6aS,6bR,8aR,10S,12aR,12bR,14bS)-10-hydroxy-2,2,6a,6b,9,9,12a-heptamethyl-1,3,4,5,6,6a,6b,7,8,8a,9,10,11,12,12a,12b,13,14b-octadecahydropicene-4a(2H)-carboxylate (**4l**)

White solid; Rf = 0.29 (cyclohexane/EtOAc, 70:30), yield 78%, 58.4 mg, mp: 112–115 °C (acetonitrile). ^{1}H-NMR (600 MHz, $CDCl_3$) δ_H 7.58 (1H, d, *J* = 9.4 Hz, H-4″), 7.32 (1H, d, *J* = 8.5 Hz, H-5″), 6.78 (1H, dd, *J* = 8.5; 2.4 Hz, H-6″), 6.75 (1H, d, *J* = 2.4 Hz, H-8″), 6.21 (1H, d, *J* = 9.4 Hz, H-3″), 5.19 (1H, t, *J* = 3.6 Hz, H-12), 4.35 (2H, m, H-1′), 4.16 (2H, m, H-2′), 3.13 (1H, m, H-3), 2.80 (1H, dd, *J* = 4.2; 13.8 Hz, H-18), 1.04 (3H, s), 0.90 (3H, s), 0.84 (3H, s), 0.82 (3H, s), 0.75 (3H, s), 0.69 (3H, s), 0.57 (3H, s). ^{13}C-NMR (150 MHz, $CDCl_3$) δ_C 177.65, 161.77 (C-7″), 161.07 (C-2″), 155.83, 143.54, 143.27 (C-4″), 129.02 (C-5″), 122.55, 113.40 (C-3″), 112.81 (C-10″), 112.74 (C-6″), 101.76 (C-8″), 78.99, 66.51 (C-2′), 62.12 (C-1′), 55.16, 47.55, 46.85, 45.81, 41.66, 41.26, 39.30, 38.73, 38.40, 36.98, 33.81, 33.07, 32.62, 32.44, 30.69, 28.10, 27.60, 27.18, 25.86, 23.60, 23.38, 22.95, 18.27, 16.99, 15.57, 15.18. ESI-HRMS calculated for $C_{41}H_{56}O_6Na$ $[M + Na]^+$: 667.3975, found: 667.3975. Δm = 0 ppm.

2-((2-Oxo-4-phenyl-2H-chromen-7-yl)oxy)ethyl(4aS,6aS,6bR,8aR,10S,12aR,12bR,14bS)-10-hydroxy-2,2,6a,6b,9,9,12a-heptamethyl-1,3,4,5,6,6a,6b,7,8,8a,9,10,11,12,12a,12b,13,14b-octadecahydropicene-4a(2H)-carboxylate (**4m**)

White solid; Rf = 0.38 (cyclohexane/EtOAc, 70:30), yield 76%, 56.7 mg, mp: 114–116 °C (acetonitrile). ^{1}H-NMR (300 MHz, $CDCl_3$) δ_H 7.51 (3H, m, H-Ar), 7.42 (2H, m, H-Ar), 7.37 (1H, d, *J* = 8.8 Hz, H-5″), 6.88 (1H, d, *J* = 2.4 Hz, H-8″), 6.78 (1H, dd, *J* = 8.8; 2.4 Hz, H-6″), 6.22 (1H, s, H-3″), 5.24 (1H, t, *J* = 3.0 Hz, H-12), 4.40 (2H, m, H-1′), 4.23 (2H, t, *J* = 4.7 Hz, H-2′), 3.19 (1H, dd, *J* = 10.5; 5.0 Hz, H-3), 2.87 (1H, dd, *J* = 13.3; 3.6 Hz, H-18), 1.10 (3H, s), 0.96 (3H, s), 0.90 (3H, s), 0.89 (3H, s), 0.80 (3H, s), 0.75 (3H, s), 0.64 (3H, s). ^{13}C-NMR (150 MHz, $CDCl_3$) δ_C 177.67, 161.72 (C-2″), 161.12 (C-7″), 155.93 (C-4″), 155.73 (C-10″), 143.53, 135.52 (C-11″), 129.66 (C-Ar), 128.88 (C-Ar), 128.36 (C-5″), 128.10 (C-Ar), 122.55, 112.85 (C-9″), 112.45 (C-3″), 112.11 (C-6″), 102.03 (C-8″), 78.98, 66.52 (C-2′), 62.12 (C-1′), 55.14, 47.54, 46.85, 45.81, 41.65, 41.26, 39.30, 38.73, 38.39, 36.97, 33.81, 33.07, 32.61, 32.44, 30.69, 28.09, 27.59, 27.16, 25.86, 23.61, 23.38, 22.95, 18.27, 15.58, 15.19. ESI-HRMS calculated for $C_{47}H_{60}O_6Na$ $[M + Na]^+$: 743.4288, found: 743.4273. Δm = −2.01 ppm.

2-((6-Methoxy-2-oxo-2H-chromen-7-yl)oxy)ethyl(4aS,6aS,6bR,8aR,10S,12aR,12bR,14bS)-10-hydroxy-2,2,6a,6b,9,9,12a-heptamethyl-1,3,4,5,6,6a,6b,7,8,8a,9,10,11,12,12a,12b,13,14b-octadecahydropicene-4a(2H)-carboxylate (**4n**)

Yellow solid; Rf = 0.62 (cyclohexane/EtOAc, 60:40), yield 78%, 58.6 mg, mp: 115–118 °C (acetonitrile). ^{1}H-NMR (500 MHz, $CDCl_3$) δ_H7.64 (1H, d, *J* = 9.4 Hz, H-4″), 6.89 (1H, s, H-5″), 6.87 (1H, s, H-8″), 6.32 (1H, d, *J* = 9.4 Hz, H-3″), 5.26 (1H, t, *J* = 3.5 Hz, H-12), 4.47 (2H, m, H-1′), 4.30 (2H, t, *J* = 5.0 Hz, H-2′), 3.92 (1H, s, H-11″), 3.21 (1H, dd, *J* = 10.0; 5.0 Hz, H-3), 2.88 (1H, dd, *J* = 13.5; 4.5 Hz, H-18), 1.12 (3H, s), 0.99 (3H, s), 0.92 (3H, s), 0.91 (3H, s), 0.82 (3H, s), 0.77 (3H, s), 0.65 (3H, s). ^{13}C-NMR (125 MHz, $CDCl_3$) δ_C 177.59, 161.28 (C-2″), 151.93 (C-6″), 149.80 (C-9″), 146.76 (C-7″), 143.51, 143.13 (C-4″), 122.55, 113.83 (C-3″), 111.88 (C-10″), 108.67 (C-5″), 101.57 (C-8″), 79.00, 67.23 (C-2′), 62.05 (C-1′), 56.44, 55.17, 47.54, 46.82, 45.79, 41.28, 39.28, 38.73, 38.42, 36.96, 33.83, 33.08, 32.59, 32.37, 30.68, 28.10, 27.59, 32.37, 27.18, 25.86, 23.58, 23.35, 22.92, 18.31, 16.93, 15.56, 15.18. ES-HRMS calculated for $C_{42}H_{58}O_7Na$ $[M + Na]^+$: 697.4080, found: 697.4070. Δm = −1.43 ppm.

3-((4-Oxo-2-phenyl-4H-chromen-6-yl)oxy)propyl(4aS,6aS,6bR,8aR,10S,12aR,12bR,14bS)-10-hydroxy-2,2,6a,6b,9,9,12a-heptamethyl-1,3,4,5,6,6a,6b,7,8,8a,9,10,11,12,12a,12b,13,14b-octadecahydropicene-4a(2H)-carboxylate (**5a**)

White solid; Rf = 0.66 (cyclohexane/EtOAc, 60:40), yield 69%, 52.1 mg, mp: 133–135 °C (EtOAc). 1H-NMR (300 MHz, $CDCl_3$) δ_H 7.94 (2H, m, H-Ar), 7.62 (1H, d, *J* = 3.0 Hz, H-8″), 7.54 (3H, m, H-Ar), 7.32 (1H, d, *J* = 3.0 Hz, H-7″), 6.85 (1H, s), 5.27 (1H, t, *J* = 3.5 Hz, H-12), 4.24 (4H, m, H-1′, 3′), 3.16 (1H, dd, *J* = 10.7; 5.3 Hz, H-3), 2.89 (1H, dd, *J* = 13.7; 4.3 Hz, H-18), 1.10 (3H, s), 0.94 (3H, s), 0.91 (3H, s), 0.89 (3H, s), 0.79 (3H, s), 0.70 (3H, s), 0.59 (3H, s). ^{13}C-NMR (150 MHz, $CDCl_3$) δ_C 177.72 (C-4″), 177.28, 163.20 (C-2″), 156.30 (C-6″), 151.17 (C-9″), 143.70, 131.79 (C-11″), 131.60 (C-Ar), 129.07 (C-Ar), 126.25 (C-Ar), 124.61 (C-10″), 124.19, 122.43 (C-7″), 119.55 (C-8″), 106.81 (C-5″), 105.31 (C-3″), 78.96, 64.65 (C-3′), 60.52 (C-1′), 55.03, 47.50, 46.75, 46.79, 41.60, 41.27, 39.10, 38.59, 38.31, 36.89, 33.83, 33.08, 32.53, 32.44, 30.69, 28.41, 27.95, 27.59, 27.10, 25.83, 23.63, 23.30, 22.94, 18.23, 16.73, 15.47, 15.16. ESI-HRMS calculated for $C_{48}H_{62}O_6Na$ $[M + Na]^+$: 757.4444, found: 757.4442. Δm = −0.26 ppm.

3-((4-Oxo-2-phenyl-4H-chromen-7-yl)oxy)propyl(4aS,6aS,6bR,8aR,10S,12aR,12bR,14bS)-10-hydroxy-2,2,6a,6b,9,9,12a-heptamethyl-1,3,4,5,6,6a,6b,7,8,8a,9,10,11,12,12a,12b,13,14b-octadecahydropicene-4a(2H)-carboxylate (**5b**)

White solid; Rf = 0.42 (cyclohexane/EtOAc, 50:50), yield 71%, 53 mg, mp: 130–133 °C (EtOAc). ^{1}H-NMR (300 MHz, $CDCl_3$) δ_H 8.17 (1H, d, *J* = 9.0 Hz, H-5″), 7.93 (1H, m, H-Ar), 7.54 (3H, m, H-Ar), 6.79 (1H, s, H-3″), 5.28 (1H, t, *J* = 3.5 Hz, H-12), 4.24 (4H, m, H-1′, 3′), 3.17 (1H, dd, *J* = 10.8; 4.8 Hz, H-3), 2.90 (1H, dd, *J* = 13.7; 3.6 Hz, H-18), 1.18 (3H, s), 0.94 (3H, s), 0.93 (3H, s), 0.91 (3H, s), 0.79 (3H, s), 0.69 (3H, s), 0.66 (3H, s). ^{13}C-NMR (150 MHz, $CDCl_3$) δ_C 177.82 (C-4″), 177.64, 163.40 (C-7″), 163.08 (C-2″), 157.94 (C-9″), 143.81, 131.86

(C-11″), 131.49 (C-14″), 129.06 (C-Ar), 127.24 (C-5″), 126.16 (C-Ar), 122.42, 117.98 (C-10″), 114.26 (C-6″), 107.54 (C-3″), 101.24 (C-8″), 78.95, 64.87 (C-3′), 60.46 (C-1′), 55.08, 47.50, 46.80, 45.97, 41.65, 41.32, 39.19, 38.63, 38.34, 36.89, 33.82, 33.07, 32.54, 32.25, 30.70, 28.33, 28.00, 27.58, 27.10, 25.85, 23.62, 23.33, 23.03, 18.20, 16.84, 15.43, 15.14. ESI-HRMS calculated for $C_{42}H_{58}O_7Na$ [M + Na]$^+$: 757.4444, found: 757.4483. Δm = 5.14 ppm.

3-(4-(Butoxycarbonyl)phenoxy)propyl(4aS,6aS,6bR,8aR,10S,12aR,12bR,14bS)-10-hydroxy-2,2,6a,6b,9,9,12a-heptamethyl-1,3,4,5,6,6a,6b,7,8,8a,9,10,11,12,12a,12b,13,14b-octadecahydropicene-4a(2H)-carboxylate (**5c**)

White solid; Rf = 0.55 (cyclohexane/EtOAc, 70:30), yield 68%, 50.8 mg, mp: 113–115 °C (cyclohexane/EtOAc). IR (ν_{max}/cm^{-1}) 3342.54 (OH), 2946.10 (CH str.), 1708.34 (2 × C=O), 1608.20 (C=C Ar). ^{1}H-NMR (500 MHz, $CDCl_3$) δ_H 8.01 (2H, dd, *J* = 6.9; 1.9 Hz, H-6″, 2″), 6.91 (2H, dd, *J* = 6.9; 1.9 Hz, H-5″, 3″), 5.26 (1H, t, *J* = 3.5 Hz, H-12), 4.40–4.00 (6H, m, H-1′, 3′, 8″), 3.20 (1H, dd, *J* = 11.0; 4.6 Hz, H-3), 2.87 (1H, dd, *J* = 13.8; 4.3 Hz, H-18), 1.11 (3H, s), 0.99 (3H, s), 0.98 (3H, s), 0.93 (3H, s), 0.91 (3H, s), 0.81 (3H, s), 0.77 (3H, s), 0.62(3H, s). ^{13}C-NMR (125 MHz, $CDCl_3$) δ_C 177.66, 166.41 (C-7″), 162.49 (C-4″), 143.78, 131.57 (C-Ar), 123.05 (C-1″), 122.43, 113.93 (C-Ar), 79.00, 64.57 (C-3′), 64.32 (C-8″), 60.60 (C-1′), 55.14, 47.56, 46.76, 45.82, 41.64, 41.30, 39.20, 38.71, 38.39, 36.95, 33.82, 33.08, 32.52, 30.85, 30.69, 28.41, 28.08, 27.59, 27.17, 25.88, 23.62, 23.34, 23.00, 19.31, 18.30, 16.82, 15.54, 15.22, 13.81. ESI-HRMS calculated for $C_{44}H_{66}O_6Na$ [M + Na]$^+$: 713.4757, found: 713.4756. Δm = −0.14 ppm.

3-(4-(Isobutoxycarbonyl)phenoxy)propyl(4aS,6aS,6bR,8aR,10S,12aR,12bR,14bS)-10-hdroxy-2,2,6a,6b,9,9,12a-heptamethyl-1,3,4,5,6,6a,6b,7,8,8a,9,10,11,12,12a,12b,13,14b-octadecahydropicene-4a(2H)-carboxylate (**5d**)

White solid; Rf = 0.51 (cyclohexane/EtOAc, 80:20), yield 75%, 56 mg, mp: 128–130 °C (EtOAc). IR (ν_{max}/cm^{-1}) 3542.81 (OH), 2945.28 (CH str.), 1717.37 (2 × C=O), 1603.28 (C=C Ar). ^{1}H-NMR (300 MHz, $CDCl_3$) δ_H 7.99 (2H, dd, *J* = 6.9; 2.0 Hz, H-6″, 2″), 6.90 (2H, dd, *J* = 6.9; 2.0 Hz, H-5″, 4″), 5.23 (1H, t, *J* = 3.5 Hz, H-12), 4.38 (2H, m, H-1′), 4.20 (1H, t, *J* = 4.8 Hz, H-3′), 4.07 (2H, d, *J* = 6.5 Hz, H-8″), 3.19 (1H, dd, *J* = 10.0; 5.0 Hz, H-3), 2.87 (1H, dd, *J* = 14.0; 4.0 Hz, H-18), 1.10 (3H, s), 1.01 (3H, s), 0.99 (3H, s), 0.96 (3H, s), 0.90 (3H, s), 0.88 (3H, s), 0.82 (3H, s), 0.75 (3H, s), 0.65 (3H, s). ^{13}C-NMR (75 MHz, $CDCl_3$) δ_C177.66, 166.22 (C-7″), 162.29 (C-4″), 143.54, 131.53 (C-6″, 2″), 123.45, 122.58 (C-1″), 114.20 (C-5″, 3″), 79.01, 70.73 (C-8″), 66.13 (C-3′), 62.29 (C-1′), 55.27, 47.63, 46.86, 46.89, 41.71, 41.35, 39.39, 38.73, 38.49, 37.03, 33.86, 33.00, 32.71, 32.46, 30.64, 28.09, 27.95, 27.65, 27.22, 26.90, 25.81, 23.58, 23.39, 23.01, 19.14 (C-10″, 11″), 18.28, 17.01, 15.50, 15.19. ESI-HRMS calculated for $C_{44}H_{66}O_6Na$ [M + Na]$^+$: 713.4757, found: 713.4396. Δm = 50 ppm.

3-((2-Oxo-2H-chromen-6-yl)oxy)propyl(4aS,6aS,6bR,8aR,10S,12aR,12bR,14bS)-10-hydroxy-2,2,6a,6b,9,9,12a-heptamethyl-1,3,4,5,6,6a,6b,7,8,8a,9,10,11,12,12a,12b,13,14b-octadecahydropicene-4a(2H)-carboxylate (**5e**)

White solid; Rf = 0.43 (cyclohexane/EtOAc, 70:30), yield 78%, 58.5 mg, mp: 115–118 °C (acetonitrile). ^{1}H-NMR (300 MHz, $CDCl_3$) δ_H 7.94 (1H, d, *J* = 9.5 Hz, H-4″), 7.28 (1H, d, *J* = 9.0 Hz, H-8″), 7.11 (1H, dd, *J* = 9.0; 2.8 Hz, H-7″), 6.93 (1H, d, *J* = 2.8 Hz, H-5″), 6.44 (1H, d, *J* = 9.5 Hz, H-3″), 5.27 (1H, t, *J* = 3.5 Hz, H-12), 4.25 (2H, m, H-1′), 4.09 (2H, t, *J* = 6.0 Hz, H-3′), 3.21 (1H, dd, *J* = 10.8; 5.4 Hz, H-3), 2.89 (1H, dd, *J* = 13.6; 4.4 Hz, H-18), 1.13 (3H, s), 0.99 (3H, s), 0.93 (3H, s), 0.92 (3H, s), 0.83 (3H, s), 0.78 (3H, s), 0.67 (3H, s). ^{13}C-NMR (75 MHz, $CDCl_3$) δ_C 177.36, 160.64 (C-6″), 155.35 (C-2″), 148.64 (C-9″), 143.80, 142.88 (C-4″), 122.42, 119.56 (C-10″), 119.23 (C-8″), 117.87 (C-7″), 117.21 (C-3″), 111.06 (C-5″), 78.95, 65,14 (C-3′), 60.62 (C-1′), 55.22, 47.60, 46.81, 45.88, 41.74, 41.41, 39.32, 38.72, 38.48, 37.00, 33.88, 33.00, 32.68, 32.56, 30.65, 28.61, 28.07, 27.66, 27.20, 25.82, 23.57, 23.37, 23.08, 18.31, 16.94, 15.48, 15.19. ESI-HRMS calculated for $C_{42}H_{58}O_6Na$ [M + Na]$^+$: 681.4131, found: 681.4131. Δm = 0 ppm.

3-((6-Methoxy-2-oxo-2H-chromen-7-yl)oxy)propyl(4aS,6aS,6bR,8aR,10S,12aR,12bR,14bS)-10-hydroxy-2,2,6a,6b,9,9,12a-heptamethyl-1,3,4,5,6,6a,6b,7,8,8a,9,10,11,12,12a,12b,13,14b-octadecahydropicene-4a(2H)-carboxylate (**5f**)

Yellow solid; Rf = 0.65 (cyclohexane/EtOAc, 60:40), yield 75%, 56 mg, mp: 114–117 °C (acetonitrile). ^{1}H-NMR (600 MHz, $CDCl_3$) δ_H 7.54 (1H, d, *J* = 9.4 Hz, H-4″), 6.78 (1H, s, H-8″), 6.75 (1H, s, H-5″), 6.22 (1H, d, *J* = 9.4 Hz, H-3″), 5.18 (1H, t, *J* = 3.5 Hz, H-12), 4.13 (2H, m, H-1′, 3′), 3.82 (1H, s, H-11″), 3.11 (1H, dd, *J* = 11.2; 4.5 Hz, H-3), 2.78 (1H, dd, *J* = 13.6; 4.3 Hz, H-18), 1.02 (3H, s), 0.88 (3H, s), 0.84 (3H, s), 0.82 (3H, s), 0.69 (3H, s), 0.67 (3H, s), 0.50 (3H, s). ^{13}C-NMR (75 MHz, $CDCl_3$) δ_C 177.53, 161.13 (C-2″), 152.31 (C-6″), 150.06 (C-9″), 146.67 (C-7″), 143.78, 143.02 (C-4″), 122.44, 113.61 (C-3″), 111.59 (C-10″), 108.81 (C-5″), 100.96 (C-8″), 78.95, 65.73 (C-3′), 60.55 (C-1′), 56.54 (C-11″), 55.17, 47.59, 46.82, 45.86, 41.61, 41.40, 39.27, 38.71, 38.42, 37.00, 33.87, 33.00, 32.63, 32.56, 30.64, 28.34, 28.08, 27.65, 27.20, 25.83, 23.57, 23.34, 23.04, 18.28, 16.87, 15.53, 15.16. ESI-HRMS calculated for $C_{43}H_{60}O_7Na$ $[M + Na]^+$: 711.4237, found: 711.4235. Δm = −0.28 ppm.

All ^{1}H, ^{13}C NMR, IR, and HRMS spectra are provided as Supplementary Materials.

2.4. Anti-Inflammatory Activity (Anti-15-LOX)

The evaluation of the anti-inflammatory potential of the synthesized derivatives was conducted by assessing their impact on the enzyme 15-lipoxygenase [28]. The aforementioned activity was then subjected to testing in a 96-well microplate. For each well, 20 µL of the compound (at a concentration of 100 µM) was combined with 150 µL of phosphate buffer (pH 7.4), 60 µL of linoleic acid, and 20 µL of enzyme. The mixture was subjected to a 30 s shaking process, followed by an incubation period at 25 °C for 10 min. Subsequently, the mixture's absorption was measured at a wavelength of 234 nm. The nordihydroguaiaretic acid NDGA at 13.22 µM was employed as a reference. The calculation of percentage inhibitory activity was performed employing the following equation:

$$\%\text{inhibition} = 100 \times (A_{blank} - A_{sample})/A_{blank}.$$

where A_{sample} is the absorbance of the molecule containing the reaction and $A_{control}$ is the absorbance of the reaction control.

2.5. Anti-Diabetic Activity (Anti-α-Glucosidase)

The inhibition potential of the novel compounds was evaluated by employing the p-nitrophenyl-α-D-glucopyranoside PNP-G assay [29], which assesses their ability to inhibit α-glucosidase. A phosphate-buffer solution was prepared at a concentration of 0.1 M and with a pH of 6.9. A volume of 50 µL of the aforementioned solution was combined with 100 µL of the α-glucosidase enzyme (1 U/mL) and 50 µL of each compound at a concentration of 100 µM. Subsequently, the mixture was incubated for a period of 10 min at a temperature of 25 °C. Then, 50 µL of PNP-G (5 mM) was added to the mixture, which was then shaken for 30 s and incubated for a further five minutes. The absorbance was determined at a wavelength of 405 nm. The measurement of percentage inhibitory activity was calculated according to the following equation:

$$\%\text{inhibition} = 100 \times (A_{blank} - A_{sample})/A_{blank}.$$

where A_{sample} is the absorbance of the molecule containing the reaction and $A_{control}$ is the absorbance of the reaction control.

2.6. Cytotoxic Activity

The anticancer activity of the synthesized compounds was assessed against two types of colon cancer cell line (HCT-116 and LS-174T). Furthermore, the toxic effect of the compounds was evaluated on human embryonic kidney cells (HEK-293).

In the present study, two distinct culture mediums were employed for the cells, namely: RPMI-1640 and DMEM with a high glucose content. Furthermore, both mediums were supplemented with additional ingredients, namely 10% of decomplemented fetal bovine serum, three antibiotics (streptomycin, gentamicin and penicillin) at a concentration of 0.5% each, and 1% non-essential amino acids. The HCT-116 cells were cultivated in RPMI-1640, while the LS-174T and HEK-293 cells were grown in DMEM. The test cells were then maintained within a humidified 37 °C incubator, with a 5% CO_2 concentration. The culture medium was monitored on a daily basis, and a change in medium was instigated when necessary. When the cells achieved 70–80% confluence, they were collected for subsequent use in assays to determine their cytotoxic potential.

The LS-174T and HEK-293 cell lines were seeded at a density of 12,000 cells per well in 96-well microplates. In contrast, the HCT-116 cell line was seeded at a density of 13,000 cells per well in 96-well microplates. The cells were then subjected to an overnight incubation at 37 °C within a controlled atmosphere incubator, containing CO_2. Then, each compound was diluted using culture medium (RPMI-1640 or high-glucose DMEM) to achieve concentrations of 100 µM and 10 µM, respectively, and then applied to the cells. Subsequently, the microplates were subjected to an incubation process at a temperature of 37 °C for 48 h. Cytotoxicity was evaluated through the use of the MTT (3-(4,5-dimethylthiazol-2-yl)-2,5-diphenyltetrazolium bromide) test [28]. Following the requisite incubation period, the medium was replaced with 50 µL of a 1 mg/mL MTT solution (Sigma-Aldrich), and the samples were incubated for a further 40 min. The MTT solution was then discarded. The process of reducing soluble yellow MTT to dark blue by mitochondrial dehydrogenase enzymes in viable cells is known as formazan crystal formation. In this experiment, 80 µL of solvent DMSO was used to dissolve the crystals. The measurement of the degree of absorption was conducted using a spectrophotometer at a wavelength of 605 nm with the aid of a microplate reader (Molecular Devices, type 680, Thermo Fisher Scientific, Vantaa, Finland). In this study, the reference employed was Tamoxifen at 100 µM.

2.7. Statistical Analysis

The experimental process involved the performance of all measurements in quadruplicate. A one-way analysis of variance (ANOVA) was performed with SPSS (version 20.0) for Windows to determine the significance of the results. Tukey's test was applied to assess statistical differences between synthesized **OA** derivatives. The linear correlation coefficient (R^2) was examined to establish the relationship among biological activities. Finally, a principal component analysis (PCA) was conducted utilizing XLSTAT (version 2024.3.0.1423) to visualize differences between all parameters. Reliability limits were set at $p \leq 0.05$.

2.8. The Process of Molecular Docking

The chemical compound structures of tamoxifen and the synthesized molecules (**2**, **3**, **4d**, **4e**, **4k**–**n** and **5d**–**f**) were generated and enhanced employing ACD (3D viewer) software (Version 2017.2.1, http://www.filefacts.com/acd3d-viewer-freeware-info, accessed on 11 November 2024), where their energies were minimized. The crystal structure of the epidermal growth factor receptor (EGFR) (PDB: 1M17) was downloaded from the RSCB data bank (https://www.rcsb.org, accessed on 11 November 2024). The protein was prepared by removing the complexed inhibitor ligand and water molecules. Then, the

polar hydrogens were added followed by appending Kollman charges. Hence, the grid box with dimensions of 72 × 44 × 60 points, spacing of 0.375 Å and focused on coordinates x: 24.21, y: 0.49, and z: 59.2, was generated based on the acarbose binding position in the target protein binding site. The molecular docking analyses of tamoxifen and the synthesized compounds (**2**, **3**, **4d**, **4e**, **4k–n** and **5d–f**) were conducted utilizing the AutoDock Vina software (v1.1.2) [30]. Molecule–enzyme interactions were drawn and explained by employing the Biovia Discovery Studio Visualizer (version 17.2.0.16349, BIOVIA, Dassault Systèmes (2017), San Diego, CA, USA).

3. Results and Discussion

3.1. Chemistry

3.1.1. Extraction of **OA** (**1**)

The extraction of compounds from medicinal plants is now a widely adopted practice in sectors such as chemistry, pharmaceuticals and biotechnology [31]. This process, which recovers active principles from plants, is an essential step in fully exploiting their therapeutic properties. However, it often proves complex and costly, posing a challenge in isolating the molecules. In response, researchers are focusing on improving extraction techniques to make them more efficient. In this context, recent studies indicate that this technique is becoming an increasingly popular method for the extraction of valuable molecules [32]. In addition, there is growing interest in olive pomace, which contains terpenoids such as oleanolic acid **OA** and maslinic acid. Several research studies have explored different methods for extracting these acids [33]. In this particular instance, the research methodology employed utilized ultrasonic extraction, a technique that has been identified as the most effective and appropriate technique to achieve the objectives of the research project [34]. This extraction method used resulted in isolation of 10.2 g of **OA** (**1**) with a yield of 0.3% (*w*/*w*).

3.1.2. Synthesis of New Derivatives

The synthesis began with the alkylation of **OA** (**1**) at the carboxyl group (COOH). This reaction was carried out using 1,2-dibromoethane/1,3-dibromopropane and potassium carbonate in DMF at room temperature, as shown in Scheme 1. The reaction produced two alkyl derivatives (**2**; *n* = 2 and **3**; *n* = 3) of **1** in 69 and 71% yield, respectively, and two dimers (**2a**; *n* = 2 and **3a**; *n* = 3) in 8 and 9% yield, respectively. The structures obtained were characterized and confirmed by ^{1}H-NMR and ^{13}C-NMR. The ^{1}H-NMR spectrum of **2** shows signals at δ_H 4.35 and 3.52, which can be attributed to the methylenes protons H-1′ and H-2′, respectively. In the case of the dimer (**2a**), the ^{1}H-NMR spectrum demonstrates the existence of a signal at δ_H 5.23 (2H), corresponding to the two ethylenic protons H-12. It should be noted that in the region 1–2 ppm of the ^{1}H-NMR spectrum, the observed signals correspond to methylene (CH_2) and methine (CH) groups within the pentacyclic skeleton of **OA**. These signals were not integrated because their high density and overlap make precise integration challenging. This is a common phenomenon for triterpenoids due to the complexity of their structure. Moreover, the ^{13}C-NMR spectrum displays two signals at δ_C 178.17 and 177.48 attributable to the carboxylic carbons. These findings are in well agreement with the literature [35,36].

On the other hand, the synthesized compounds, **4a–n** and **5a–f** were produced by reacting compound **2** and **3** in DMF with various polyphenols and coumarins in the presence of caesium carbonate. This reaction yielded products in yields ranging from 68 to 79%, as illustrated in Scheme 1. The structures of compounds **4a–n** and **5a–f** were confirmed by ^{1}H-NMR, ^{13}C-NMR and HRMS.

3.2. Biological Activity

3.2.1. Anti-15-Lipoxygenase Activity

Anti-inflammatory properties of the synthesized molecules were evaluated at a concentration of 100 µM against the enzyme 15-lipoxygenase. NDGA at a concentration 13.22 µM was employed as a positive control under identical conditions. The results presented in Table 1 show that most of the compounds synthesized have no anti-inflammatory activity. Statistical analysis revealed a significant difference ($p \leq 0.05$) between compound **1** and its derivatives with regard to this activity. However, compounds **4f**, **4g**, **4j**, **4l** and **5e** demonstrated a low degree of inhibition of the 15-LOX enzyme, with inhibition percentages not exceeding 24.0%. It is noteworthy that compound **4i** demonstrated a moderate inhibitory effect of 32.2%, which may be attributed to the presence of α-tocopherol (vitamin E), which has been shown to inhibit the 15-LOX enzyme. The alkylation of compound **1** resulted in an increase in inhibitory potency, with a percentage of inhibition of 22.6 and 86.7%, respectively. Furthermore, the higher activity of derivatives **2** and **3** in comparison to compound **1** and the other derivatives indicated that the bromine atom made a significant contribution to this activity. Moreover, in comparison with the other derivatives, dimers **2a** and **3a** exhibited a significant inhibitory effect, with inhibition percentages of 83.1 and 39.8%, respectively, against 15-LOX. This noteworthy activity can be attributed to the presence of two **OA** (**1**) molecules.

Table 1. Anti-15-Lipoxygenase and anti-α-Glucosidase activities of **OA** (**1**) and its derivatives at 100 µM. Different letters in columns indicate significant differences according to Tukey's test ($p \leq 0.05$).

Compounds	Anti-15-Lipoxygenase		Anti-α-Glucosidase	
	Inhibition (%)	IC_{50} (µM)	Inhibition (%)	IC_{50} (µM)
1 (OA)	na	-	11.5 ± 3.6^{g}	-
2	22.6 ± 15.7^{b}	-	10.9 ± 1.1^{g}	-
2a	83.1 ± 18.3^{a}	52.4 ± 16.1	61.5 ± 4.1^{a}	59.5 ± 10.8
3	86.7 ± 14.1^{a}	29.0 ± 14.7	13.8 ± 2.5^{g}	-
3a	39.8 ± 9.6^{b}	-	54.3 ± 12.5^{a}	-
4a	11.5 ± 1.1^{d}	-	11.5 ± 1.1^{g}	-
4b	na	-	23.0 ± 1.4^{f}	-
4c	na	-	na	-
4d	na	-	4.1 ± 4.5^{h}	-
4e	na	-	na	-
4f	7.0 ± 2.0^{d}	-	na	-
4g	na	-	4.5 ± 3.1^{h}	-
4h	na	-	39.9 ± 7.1^{c}	-
4i	na	-	na	-
4j	18.8 ± 6.6^{c}	-	12.5 ± 4.6^{g}	-
4k	na	-	35.5 ± 3.5^{e}	-
4l	7.8 ± 5.3^{d}	-	11.2 ± 1.6^{g}	-
4m	na	-	43.7 ± 2.1^{b}	-
4n	na	-	10.7 ± 4.0^{g}	-
5a	na	-	2.7 ± 5.5^{h}	-
5b	na	-	57.7 ± 11.5^{a}	-
5c	na	-	39.8 ± 5.8^{d}	-
5d	na	-	na	-
5e	24.0 ± 4.6^{b}	-	38.0 ± 3.0^{e}	-
5f	na	-	54.6 ± 3.4^{a}	-
NDGA	84.7 ± 1.8	-	-	-
Acarbose	-	-	75.3 ± 0.4	-

IC_{50}: inhibitory concentration required for 50% inhibition; na: not active. NDGA: was used as reference at 13.22 µM. Acarbose: was used as reference at 77.45 µM. Data are the mean of three repetition ± SD. The different letters (**a**–**h**) indicate a significant difference between the **OA** and their derivatives ($p \leq 0.05$).

3.2.2. Anti-α-Glucosidase Activity

The anti-diabetic potential of the synthesized compounds was determined at a concentration of 100 µM using the α-glucosidase assay, with acarbose employed as the positive control. As illustrated in Table 1, the data demonstrate that 19 of the 24 compounds exhibit moderate and low inhibitory activity against α-glucosidase, with inhibition percentages ranging from 4.1 to 57.7%. A significant difference was observed between **OA** (**1**) and some of its derivatives. At a concentration of 100 µM, the two dimers (**2a** and **3a**) showed significant inhibitory activity, surpassing that of **OA** (**1**) with inhibition rates of 61.5 and 54.3%, respectively. The transformation of compound (**1**) into a dimer resulted in a notable enhancement of its anti-diabetic efficacy [37]. On the other hand, compounds **4k**, **4m**, **5e** and **5f**, which contain a coumarin motif, demonstrated moderate yet slightly elevated inhibition compared to **OA** (**1**) (11.5%), with inhibition rates of 35.5, 43.7, 38.8 and 54.6%, respectively. The discrepancy in inhibitory activity observed between compounds **4k** and **4l**, which diverged only in the position of the hydroxyl group at the B-ring of coumarin, suggests that the hydroxyl position at C-6 may confer a greater potential for activity than the C-7 position. Moreover, the difference in inhibition between compounds **4k** (35.5%) and **4m** (43.7%) can be attributed to the existence of a phenyl group at the A-ring of coumarin.

These findings are consistent with previous literature, which has demonstrated the α-glucosidase inhibitory activity of coumarin derivatives [38,39]. Furthermore, the comparison between the new **4a**–**n** (n = 2) and **5a**–**f** (n = 3) derivatives demonstrates that there is no significant difference in their anti-α-glucosidase activity.

3.2.3. Cytotoxicity Evaluation

The anticancer activity results obtained from the MTT test are of interest and provide a positive outlook for further research. The MTT test was utilized to evaluate the antiproliferative impact of compound **1** and its derivatives following a 48 h treatment period on two tumour lines (HCT-116 and LS-174T) and non-tumour cells (HEK-293), in comparison with tamoxifen at a concentration of 100 µM. As demonstrated in Figure 2 and Table 2, the results indicate that **1** exhibit comparatively low inhibitory potential at a concentration of 100 µM in the HCT-116 and LS-174T cell lines, with inhibitions of 21.2 and 32.3%, respectively. In contrast, no inhibitory activity was observed against HEK-293 cells. The dimers (**2a**) and (**3a**) were observed to exert a moderate effect against the cell lines [40]. In a study conducted by Günther et al. [41], **OA** dimers were observed to exhibit anticancer activity against SKBR-3, SKOV-3, PC-3 and U-87 cell lines. In contrast, derivatives **2** and **3** demonstrated promising anticancer activity, particularly against LS-174T cells, with 59.5 and 62.4% inhibition, respectively, and an IC_{50} value of 55.3 and 55.0 µM, respectively. The results demonstrated with clarity the contribution of the bromine atom to the enhancement of the cytotoxic activity of the **OA** (**1**).

Nevertheless, the efficacy of **OA** (**1**) can be significantly enhanced through structural modifications, particularly through the introduction of phenolic and coumarin groups. The majority of polyphenol compounds, identified under numbers **4a** to **4j** and **5a** to **5d**, show a significant inhibition. For example, compound **4d** demonstrated inhibitory activity against HCT-116 cells, with an IC_{50} of 38.5 µM, and 33.2% inhibition against LS-174T cells. In contrast, derivative **4c** exhibited minimal inhibition, highlighting the significance of the aromatic group in enhancing the inhibition of these two cell lines. Additionally, compound **4e** demonstrated significant inhibitory activity against the colon cancer cell lines (HCT-116 and LS-174T) with 55.9 and 65.3%, respectively. A comparison of the activity of compounds **4a**, **4b** and **4c** against HCT-116 cells demonstrated a gradual decline in activity, 51.51, 34.06 and 18.45%, respectively. These observations suggest that the length of the hydrocarbon

chain in the incorporated fragments may exert an influence on the inhibitory effect observed against HCT-116.

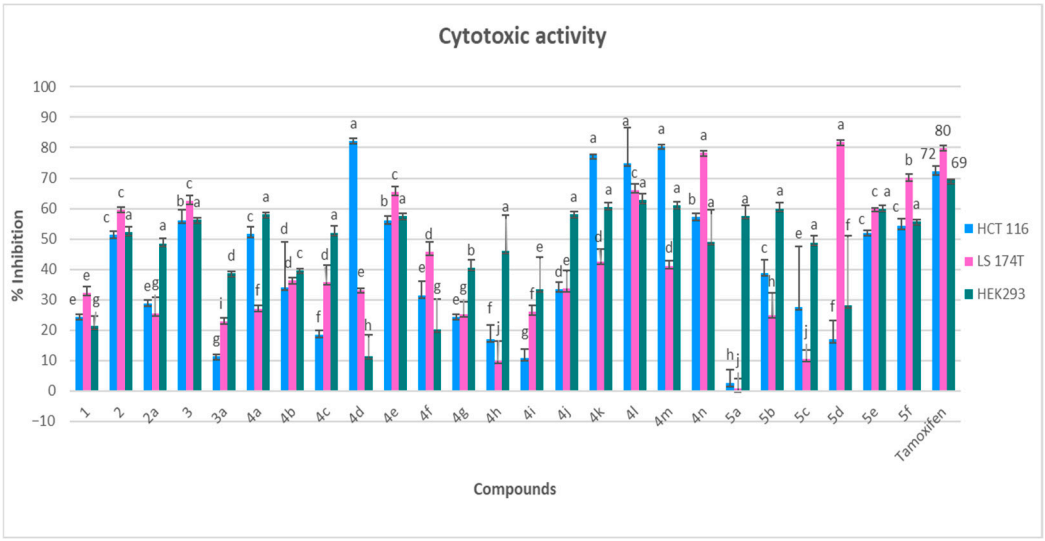

Figure 2. Cytotoxic activity of **OA** (**1**), their derivatives and Tamoxifen (100 µM) against the HCT-116, LS-174T and HEK-293 cancer cell lines. Different letters (**a**–**j**) indicate significant differences according to Tukey's test ($p \leq 0.05$).

Table 2. IC_{50} of the cytotoxic activity of **OA** (**1**) and its derivatives.

Compounds	IC_{50} (µM)		
	HCT-116	**LS-174T**	**HEK-293**
1 (OA)	-	-	-
2	-	55.3 ± 5.0	-
2a	-	-	-
3	-	55.0 ± 4.0	80.7 ± 2.6
3a	-	-	-
4a	-	-	79.1 ± 0.6
4b	-	-	-
4c	-	-	-
4d	38.5 ± 1.7	-	-
4e	-	44.3 ± 3.9	78.2 ± 1.3
4f	-	-	-
4g	-	-	-
4h	-	-	-
4i	-	-	-
4j	-	-	69.3 ± 2.3
4k	39.3 ± 2.9	-	59.2 ± 3.5
4l	43.0 ± 14.4	44.0 ± 5.6	53.5 ± 5.3
4m	40.0 ± 0.1	-	66.7 ± 3.8
4n	71.5 ± 4.8	37.2 ± 2.5	-
5a	-	-	78.6 ± 8.2
5b	-	-	42.2 ± 6.6
5c	-	-	-
5d	-	38.0 ± 1.5	-
5e	-	54.9 ± 7.8	69.9 ± 0.7
5f	-	41.8 ± 1.5	81.1 ± 5.4
Tamoxifen	35.0 ± 3.0	30.9 ± 1.6	39.6 ± 5.6

IC_{50}: inhibitory concentration required for 50% inhibition. Data are the mean of three repetition ± SD.

The inhibitory effect of Compound **5d** was found to be significant, with an IC_{50} value of 38.0 μM and an inhibition rate of 81.8%. These results are in accordance with the observations made by Karjalainen et al. [42], who demonstrated that polyphenols can enhance anti-tumour activity. The cytotoxic effect of the molecules synthesized demonstrated the significance of the fragments added to the compound **1** via the ethylene and propylene groups in inducing cytotoxic activity. This finding supports previous research that has shown the efficacy of coumarin derivatives in cancer treatment [43,44].

In particular, compounds **4k**, **4l**, **4m**, **4n**, **5e** and **5f** which contain coumarin groups, demonstrated notable inhibitory activity. Of these, compounds **4k** and **4m** demonstrated the greatest inhibitory capacity, with IC_{50} values of 39.3 and 40.0 μM, respectively, and the ability to inhibit 77.3 and 80.4% of HCT-116 cells, respectively. These values were slightly higher than those observed for compounds **4l** and **4n**. In LS-174T cells, however, compounds **4l** and **4n** demonstrated higher inhibitory activity, reaching 66.0 (IC_{50} = 44.0 μM) and 78.3% (IC_{50} = 37.3 μM), respectively. In contrast, compounds **4k** and **4m** exhibited minimal inhibitory activity. In conclusion, coumarins with a hydroxyl group at C-6 have been demonstrated to exhibit notable anticancer activity against HCT-116 cells, whereas those with a hydroxyl group at C-7 have been shown to display particular efficacy against LS-174T cells. The results obtained are in accordance with the observations of Martínez-Lara et al. [45], who found that the derivation of **OA** (**1**) with coumarin increased anticancer efficacy, thus demonstrating the augmented therapeutic potential of compounds modified with these groups. However, the form in which coumarin is attached to a molecule is likely to influence its cytotoxic activity, as previous research has shown that coumarin fragments have anticancer properties against colon cells [46].

It is interesting to note that all the compounds tested exhibited non-toxic effects on normal cells with IC_{50} values range widely from 53.5 to 81.1 μM, in contrast to the effects observed with tamoxifen, which exhibited higher levels of inhibition on these normal cells (IC_{50} = 39.6 μM). This observation highlights the importance of evaluating the specificity and toxicity of anticancer compounds and their impact on non-cancerous cells, in order to prevent adverse effects.

Statistically significant differences were not detected between compound **1** and some of its derivatives with regard to their capacity to inhibit the cells under investigation. On the other hand, significant differences were observed between the various derivatives themselves, highlighting the influence of structural modifications on their cytotoxic activity. In conclusion, the incorporation of phenolic groups and coumarins into the structure of compound **1** enhanced its inhibitory activity, highlighting the importance of structural modifications in improving therapeutic efficacy against cancer cells. These derivatives showed more marked inhibition of tumour cell lines, while retaining more moderate activity on non-tumour cell lines, suggesting significant selectivity. Therefore, these observations confirm that certain structural modifications make it possible to target tumour cells more specifically, reinforcing the therapeutic potential of these derivatives in a targeted and effective approach. It remains essential to maintain a balance between these improvements and to carry out a complete assessment of specificity and toxicity in order to guarantee the safety of the treatments developed.

3.3. Principal Component Analysis (PCA)

In this study, a principal component analysis (PCA) was carried out to identify the correlation between **OA** (**1**) and its derivatives and the various biological tests, with the objective of simplifying the data and identifying compounds with strong anti-15-LOX, anti-α-glucosidase and anticancer potential (Table 3). All axes of measurement were excluded from the results obtained.

Table 3. Contributions of variables (%).

	F1	F2
Anti-15-Lipoxygenase	0.298	18.814
Anti-α-Glucosidase	3.910	44.534
HCT-116	43.586	3.445
LS-174T	28.653	17.621
HEK-293	23.553	15.586

As shown in Figure 3, the percentage of total variation was established at 61.22%. The first and second principal components (PC1 and PC2) accounted for 31.27 and 28.96% of the total variability, respectively.

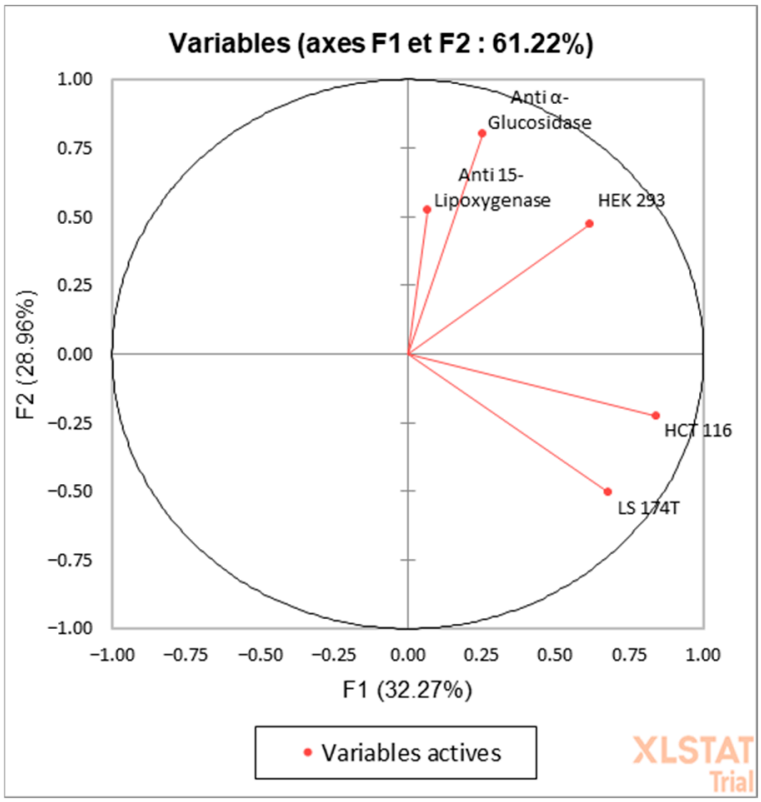

Figure 3. Principal component analysis "loading plot" of biological activities (anti-inflammatory activity: anti-15-LOX), (antidiabetic activity: anti-α-glucosidase) and the cytotoxic activity (HCT-116, LS-174T and HEK-293) of the new derivatives of **OA** (**1**).

Referring to the data in Table 4, many correlations were identified. PC1 was found to be positively correlated with the cytotoxic activity of HCT-116, LS-174T, and HEK-293, with correlation coefficients of 0.839, 0.680, and 0.616, respectively. Moreover, the second PC2 exhibited a positive correlation with the level of anti-inflammatory activity (15-LOX) and α-glucosidase (0.522 and 0.803, respectively) and a negative correlation with the cytotoxic activity against HCT-116 and LS-174T ($r = -0.223$ and $r = -0.505$).

Table 4. Correlations between variables and factors.

	F1	F2
Anti-15-Lipoxygenase	0.069	0.522
Anti-α-Glucosidase	0.251	0.803
HCT-116	0.839	−0.223
LS-174T	0.680	−0.505
HEK-293	0.616	0.475

In the biplot (Figure 4), the molecules are positioned according to their biological activities, which reveals that **OA** (**1**) displays no marked activity against α-glucosidase and 15-lipoxygenase. This limits its ability to be used in the control of diabetes. In contrast, derivative **4a** exhibited robust anti-α-glucosidase and anti-15-lipoxygenase activities, while derivatives **4f** and **4m** demonstrated pronounced cytotoxicity against cancer cells. These findings suggest that structural modifications of **OA** derivatives could enhance their therapeutic efficacy. Furthermore, the presence of functional groups, such as those associated with coumarin, could augment these effects [45].

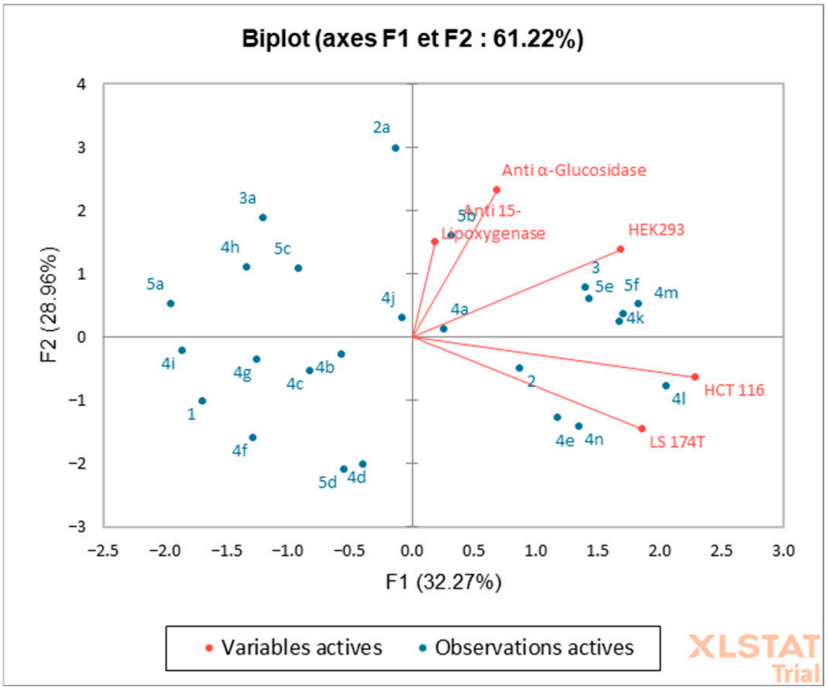

Figure 4. Principal component analysis (PCA) "Biplot" of derivatives and biological activities (anti-inflammatory activity: anti-15-LOX); (antidiabetic activity: anti-α-glucosidase); (cytotoxic activity: HCT-116, LS-174T and HEK-293).

3.4. Molecular Docking Analysis for Cytotoxic Activity (PDB: 1M17)

The EGFR is a critical receptor tyrosine kinase that plays a fundamental role in cellular processes, including growth, differentiation, metabolism, adhesion, motility, and apoptosis [47–49]. EGFR overexpression has been implicated in the pathogenesis of various human malignancies, including colorectal, lung, and breast cancers [50]. Due to its critical role in oncogenic signalling, EGFR has emerged as a prominent therapeutic target in cancer treatment strategies.

Molecular docking of the synthesized molecules (**2**, **3**, **4d**, **4e**, **4k**–**n** and **5d**–**f**) and tamoxifen (the standard inhibitor) within the ATP binding site of EGFR (protein data bank ID: 1M17) was conducted to gain insight into the binding mode and rationalize the observed in vitro cytotoxic activity. The binding energies and interaction details (number of interactions, sum of interactions between amino acids, and interactions between amino acids and hydrogen bonds) of the ligands with the target enzyme are presented in Table 5.

The positioning of all the synthesized compounds within the active site of EGFR was found to be optimal, with the resultant scores and interaction binding at the amino acids in the receptor pocket exhibiting a high degree of variability. In silico docking analysis (Table 5) revealed that the tested compounds (**2**, **3**, **4d**, **4e**, **4k**–**n** and **5d**–**f**) demonstrated promising binding scores, ranging from −8.4 to −11.6 kcal/mol, which were notably better than that of tamoxifen (−7.3 kcal/mol). The results of this study indicate that the compounds under investigation have the potential to bind with a higher degree of affinity to the active site of the EGFR enzyme in comparison to tamoxifen.

Table 5. Binding energy (kcal/mol) and interaction specifics of derivatives **2**, **3**, **4d**, **4e**, **4k**–**n**, **5d**–**f** and tamoxifen docked in the active site of EGFR enzyme (PDB: 1M17).

Compounds	Binding Energy (kcal/mol)	Interaction Detail: NI/NIAA: IAA
2	−8.9	13/6: LEU-694, PHE-699, VAL-702, ALA-719,CYS-773*, LEU-820
3	−8.4	16/9: LEU-694, PHE-699, VAL-702, ALA-719, LYS-721, THR-766*, CYS-773, LEU-820, THR-830
4d	−10.1	15/9: PHE-699, VAL-702, LYS-721, ILE-735, GLU-738, THR-766*, CYS-773, LEU-820, ASP-831
4e	−9.5	17/10: LEU-694, PHE-699, VAL-702, ALA-719, LYS-721, THR-766*, GLY-772, CYS-773, LEU-820, THR-830
4k	−10.2	15/7: PHE-699, VAL-702, LYS-721, THR-766*, ARG-817, LEU-820, ASP-831
4l	−10.5	16/9: LEU-694, PHE-699, VAL-702, ALA-719, LYS-721, THR-766*, MET-769*, CYS-773, LEU-820
4m	−11.6	19/12: LEU-694, PHE-699, VAL-702, ALA-719, LYS-721, MET-769*, CYS-773, LEU-775, ARG-817, LEU-820, LEU-834, LYS-851*
4n	−9.2	16/8: PHE-699, VAL-702, LYS-721*, THR-766*, CYS-773, ARG-817*, LEU-820, ASP-831
5d	−9.6	11/6: PHE-699, VAL-702, LYS-721, THR-766*, LEU-820, LEU-834
5e	−9.0	11/8: LEU-694, PHE-699, VAL-702, MET-769*, CYS-773, LEU-775, ARG-817, LEU-820
5f	−9.4	16/10: PHE-699, VAL-702, ALA-719, MET-769*, CYS-773, LEU-775, ARG-817, LEU-820, ASP-831, LYS-851*
Tamoxifen	−7.3	9/8: LEU-694, PHE-699, VAL-702, GLU-738, CYS-773, LEU-820, THR-830*,ASP-831

NI: Number of interactions; NIAA: Number of interacting amino acids; IAA: Interacting amino acids; * = One hydrogen bond.

As shown in Table 6, compounds **4d**, **4e**, **4k**–**m** and **5d** exhibiting lower binding energies (−10.1, −9.5, −10.2, −10.5, −11.6 and −9.6 kcal/mol, respectively), demonstrated binding modes quite similar to that of tamoxifen (binding energy = −7.3 kcal/mol). Tamoxifen was stabilized within the EGFR pocket via a hydrogen bond formation with THR-830 residue with the bond length of 2.95 Å. Furthermore, it formed a carbon hydrogen bond

with GLU-738 (bond length: 3.46 Å), a Pi–anion bond with ASP-831 (bond length: 4.31 Å), a Pi–sulfur bond with CYS-773 (bond length: 5.81 Å), a Pi–Pi Stacked bond with PHE-699 (bond length: 4.01 Å) and four Pi–alkyl bonds with LEU-694 (bond length: 5.20), PHE-699 (bond length: 5.02), VAL-702 (bond length: 4.96) and LEU-820 (bond length: 4.78 Å). On another side, the compound **4d** fitted inside the binding site of the EGFR by a hydrogen bond formation, with THR-766 (bond length: 2.91 Å), with an additional two Pi–anion interactions with GLU-738 (bond length: 3.77 Å), ASP-831 (bond length: 3.46 Å),ten alkyl bonds with VAL-702 (bonds length: 3.85, 4.11, 4.21 and 4.49 Å), LYS-721 (bond length: 3.69 Å), CYS-773 (bond length: 5.13 Å) and LEU-820 (bonds length: 3.91, 4.82 and 5.35 Å) residues, and two Pi–alkyl bonds with PHE-699 (bonds length: 4.97 and 5.36 Å). Moreover, the compound **4e** formed a hydrogen bond with THR-766 at 2.88 Å, two carbon hydrogen bonds with GLY-772 and THR-830at 3.71 and 3.64 Å, respectively, twelve alkyl bonds with LEU-694, VAL-702, ALA-719, LYS-721, CYS-773 and LEU-820 at 4.54, 3.44, 3.47, 4.55, 4.91, 5.39, 3.80, 3.84, 4.55, 5.16, 4.65 and 5.07 Å, respectively, and two Pi–alkyl bonds with PHE-699 at 4.78 and 5.17 Å. The compound **4k** showed a hydrogen bond with the THR-766 (bond length: 2.52 Å) amino acid. Also, it showed two Pi–anion interactions with ASP-831 (bonds length: 3.38 and 4.06 Å), two Pi–Pi Stacked bonds with PHE-699 (bonds length: 4.33 and 5.86 Å), nine alkyl bonds with VAL-702 (bonds length: 3.71, 3.79, 3.90, 4.69 and 5.12 Å), LYS-721 (bond length: 3.86 Å), ARG-817 (bond length: 5.43 Å), and LEU-820 (bonds length: 4.06 and 4.60 Å) residues and a Pi–alkyl bond with PHE-699 (bond length: 5.06 Å). The compound **4l**, was engaged in two hydrogen bonds, two Pi–sigma interactions, ten alkyl bonds and two Pi–alkyl bonds with residues THR-766 (bond length: 2.51 Å), MET-769 (bond length: 3.23 Å), LEU-694 (bonds length: 3.30 and 3.96 Å), VAL-702 (bonds length: 3.32, 3.36, 4.39 and 4.80Å), ALA-719 (bond length: 3.60 Å), LYS-721 (bonds length: 3.99 and 4.61 Å), CYS-773 (bond length: 5.15 Å), LEU-820 (bonds length: 4.62 and 5.02 Å) and PHE-699 (bonds length: 4.96 and 5.26 Å), respectively. The compound **4m** formed two hydrogen bonds with MET-769 (bond length: 2.96Å) and LYS-851 (bond length: 2.05 Å), a Pi–sigma interaction with VAL-702 (bond length: 3.08 Å), fourteen alkyl bonds with LEU-694 (bonds length: 5.04 and 5.31 Å),VAL-702 (bonds length: 4.80 and 5.05 Å), ALA-719 (bonds length: 4.50 and 5.07 Å), LYS-721 (bond length: 4.82 Å), CYS-773 (bonds length: 4.51 and 4.76 Å), LEU-775 (bond length: 5.12 Å), ARG-817 (bonds length: 4.25 and 4.71 Å), LEU-820 (bond length: 4.92 Å), and LEU-834 (bond length: 4.75 Å) and two Pi–alkyl bonds with PHE-699 (bonds length: 4.67 and 5.08 Å). The compound **5d** interacts with in many amino acids of the active site of EGFR via a hydrogen bond, a Pi–Pi Stacked bond, eight alkyl bonds and a Pi–alkyl bond with the side chain residues THR-766 (bond length: 2.25 Å), PHE-699 (bond length: 4.49 Å), VAL-702 (bonds length: 3.75, 3.77, 3.93 and 5.11 Å), LYS-721 (bond length: 4.04 Å), LEU-820 (bonds length: 3.99 and 4. 37 Å), LEU-834 (bond length: 4.94 Å), PHE-699 (bond length: 5.24 Å), respectively.

Although this study shows promising anticancer activity against the HCT-116 and LS-174T cell lines, it is important to note that there are no in vivo studies to confirm the efficacy of these compounds in a more complex biological context. In addition, although a preliminary toxicity profile has been assessed in healthy HEK cells, it remains insufficient to assess the safety of the compounds for clinical use. These limitations highlight the need for further research, including in vivo studies and detailed toxicity assessments, to fully establish the therapeutic potential and safety of these compounds before clinical applications can be considered.

Table 6. Three-dimensional representations showing the binding interactions and positioning of the compounds **4d**, **4e**, **4k–m**, **5d** and tamoxifen inside the binding pocket of EGFR enzyme.

Compounds	3D Binding Interactions	3D Pocket Positioning
4d	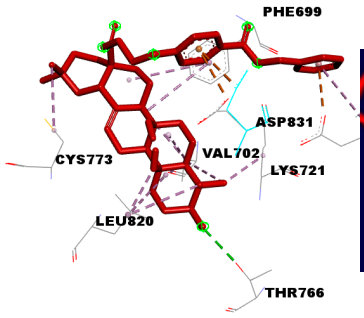	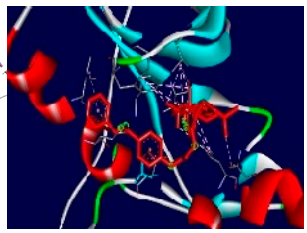
4e	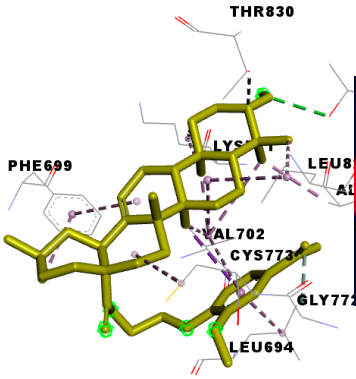	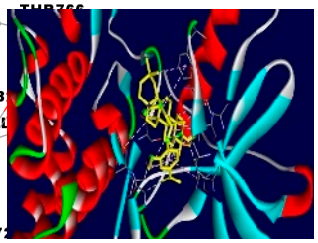
4k	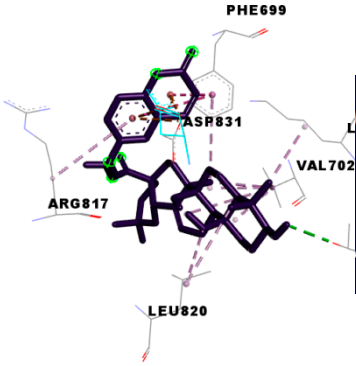	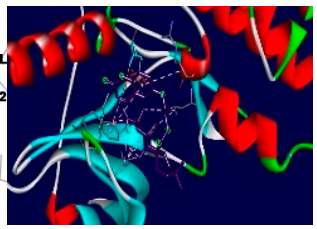
4l	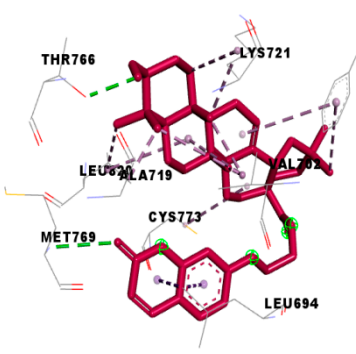	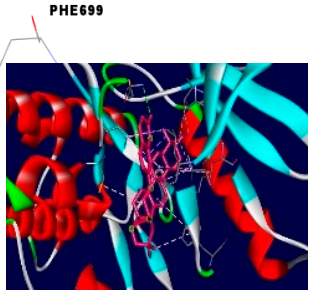

Table 6. *Cont.*

Compounds	3D Binding Interactions	3D Pocket Positioning
4m	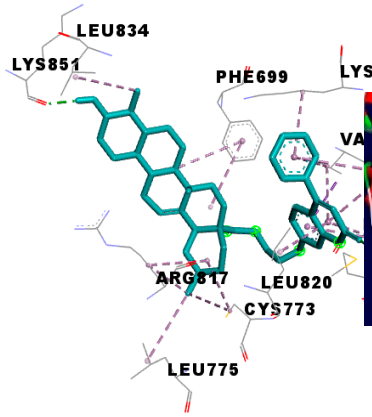	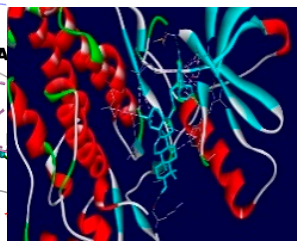
5d	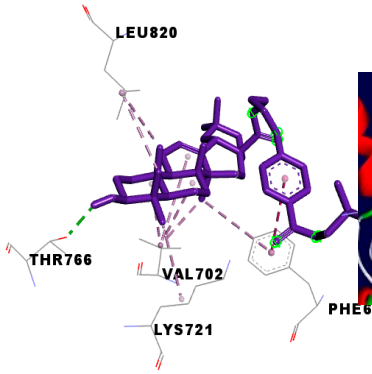	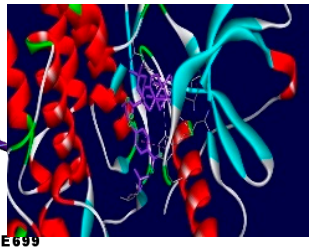
Tamoxifen	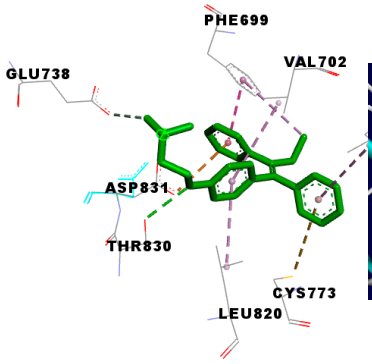	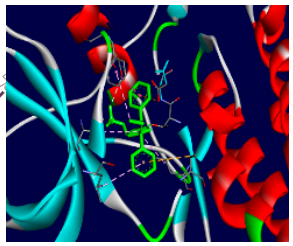

4. Conclusions

In this study, we present the valorization of **OA** (**1**), a natural bioactive pentacyclic triterpenoid, through the semi-synthesis of new compounds, as well as an evaluation of their inhibitory activity on 15-lipoxygenase, α-glucosidase, and their anticancer potential against HCT-116, LS-174T, and HEK-293 cell lines. **OA** (**1**) was extracted from olive pomace (*O. europaea*) using an ultrasonication method. The biological studies of the synthetic derivatives revealed a weak inhibitory activity on 15-LOX, accompanied by a slightly increased anti-α-glucosidase activity. In contrast, the majority of these compounds exhibited enhanced anticancer activity relative to the starting **OA** (**1**). Derivatives **4d**, **4k**, **4l**, **4m**, **4n**, **5e**, and **5f** showed considerable inhibitory activity against the HCT-116 line, while compounds **4e**, **4l**, **4n**, **5d**, **5e**, and **5f** exhibited comparable inhibitory activity against the LS-174T line. These results indicate that the majority of the semi-synthesized compounds possess a highly promising cytotoxic profile when compared to the starting acid. In silico analysis corroborated the in vitro cytotoxic activity, revealing that the synthesized molecules (**2**, **3**,

4d, **4e**, **4k**–**n**, and **5d**–**f**) exhibited strong interactions within the ATP-binding site of EGFR (Protein Data Bank ID: 1M17).

Supplementary Materials: The following supporting information can be downloaded at: https://www.mdpi.com/article/10.3390/chemistry7020036/s1, NMR, IR and HRMS spectra of the synthesized compounds.

Author Contributions: Methodology, M.Z., H.B.J. and J.B.; Software, S.J.; Validation, M.Z., H.B.J. and J.B.; Formal analysis, N.T.; Data curation, S.J.; Writing—original draft, N.T.; Writing—review & editing, S.J.; Supervision, M.Z. and J.B.; Project administration, H.B.J. and J.B.; Funding acquisition, H.B.J. and J.B. All authors have read and agreed to the published version of the manuscript.

Funding: This research was funded by Campus France and the Ministry of Higher Education and Scientific Research of Tunisia through the Hubert Curien-Utique programme PHC-UTIQUE PROJECT: 22G1202.

Data Availability Statement: The original contributions presented in this study are included in the article/Supplementary Material. Further inquiries can be directed to the corresponding author.

Conflicts of Interest: The authors affirm that there are no conflicts of interest to declare.

Abbreviations

^{1}H-NMR	proton nuclear magnetic resonance
^{13}C-NMR	carbon nuclear magnetic resonance
HRMS	high-resolution mass spectrometry
TNF-α	tumour necrosis factor α
IL-6	Interleukin-6
NDGA	nordihydroguaiaretic acid
PNP-G	p-nitrophenyl-α-D-glucopyranoside

References

1. Natalucci, V.; Marmondi, F.; Biraghi, M.; Bonato, M. The Effectiveness of Wearable Devices in Non-Communicable Diseases to Manage Physical Activity and Nutrition: Where We Are? *Nutrients* **2023**, *15*, 913. [CrossRef] [PubMed]
2. Ding, D.; Lawson, K.D.; Kolbe-Alexander, T.L.; Finkelstein, E.A.; Katzmarzyk, P.T.; Van Mechelen, W.; Pratt, M. The Economic Burden of Physical Inactivity: A Global Analysis of Major Non-Communicable Diseases. *Lancet* **2016**, *388*, 1311–1324. [CrossRef] [PubMed]
3. Asiminicesei, D.-M.; Fertu, D.I.; Gavrilescu, M. Impact of Heavy Metal Pollution in the Environment on the Metabolic Profile of Medicinal Plants and Their Therapeutic Potential. *Plants* **2024**, *13*, 913. [CrossRef]
4. Ouedraogo, W.J.; Yerbanga, R.S.; Meda, R.; Ouedraogo, J.B.; Ouedraogo, A.G. Revue Des Plantes Médicinales à Potentiel Aromatique Du Burkina Faso. *Health Res. Afr.* **2024**, *2*, 1–14.
5. Aly, S.H.; Elbadry, A.M.M.; Doghish, A.S.; El-Nashar, H.A.S. Unveiling the Pharmacological Potential of Plant Triterpenoids in Breast Cancer Management: An Updated Review. *Naunyn Schmiedebergs Arch. Pharmacol.* **2024**, *397*, 5571–5596. [CrossRef] [PubMed]
6. Liu, J.; Yin, X.; Kou, C.; Thimmappa, R.; Hua, X.; Xue, Z. Classification, Biosynthesis and Biological Function of Triterpene Esters in Plants. *Plant Commun.* **2024**, *5*, 100845. [CrossRef]
7. Triaa, N.; Znati, M.; Ben Jannet, H.; Bouajila, J. Biological Activities of Novel Oleanolic Acid Derivatives from Bioconversion and Semi-Synthesis. *Molecules* **2024**, *29*, 3091. [CrossRef]
8. Feng, A.; Yang, S.; Sun, Y.; Zhang, L.; Bo, F.; Li, L. Development and Evaluation of Oleanolic Acid Dosage Forms and Its Derivatives. *BioMed Res. Int.* **2020**, *2020*, 1308749. [CrossRef]
9. Verma, N.; Raghuvanshi, D.S.; Singh, R.V. Recent Advances in the Chemistry and Biology of Oleanolic Acid and Its Derivatives. *Eur. J. Med. Chem.* **2024**, *276*, 116619. [CrossRef]
10. Şenol, H.; Ghaffari-Moghaddam, M.; Bulut, Ş.; Akbaş, F.; Köse, A.; Topçu, G. Synthesis and Anticancer Activity of Novel Derivatives of α, β-Unsaturated Ketones Based on Oleanolic Acid: In Vitro and in Silico Studies against Prostate Cancer Cells. *Chem. Biodivers.* **2023**, *20*, e202301089. [CrossRef]

11. Kazakova, O.B.; Rubanik, L.V.; Petrova, A.V.; Smirnova, I.E.; Terekhova, A.V.; Baikova, I.P. Synthesis and Antichlamydial Activity of Oleanolic Acid Aza-Derivatives. *Chem. Nat. Compd.* **2024**, *60*, 84–91. [CrossRef]
12. Xiaofei, J.; Mingqing, S.; Miao, S.; Yizhen, Y.; Shuang, Z.; Qinhua, X.; Kai, Z. Oleanolic Acid Inhibits Cervical Cancer Hela Cell Proliferation through Modulation of the ACSL4 Ferroptosis Signaling Pathway. *Biochem. Biophys. Res. Commun.* **2021**, *545*, 81–88. [CrossRef]
13. Yang, Y.-H.; Dai, S.-Y.; Deng, F.-H.; Peng, L.-H.; Li, C.; Pei, Y.-H. Recent Advances in Medicinal Chemistry of Oleanolic Acid Derivatives. *Phytochemistry* **2022**, *203*, 113397. [CrossRef]
14. Gao, C.-X.; Tang, C.-H.; Wu, T.-J.; Hu, Y.; Peng, Y.-L.; Liu, M.-L.; Liu, Q.-W.; Chen, H.-F.; Yang, Z.-H.; Zheng, X. Anticancer Activity of Oleanolic Acid and Its Derivatives Modified at A-Ring and C-28 Position. *J. Asian Nat. Prod. Res.* **2023**, *25*, 581–594. [CrossRef] [PubMed]
15. Prabhu, S.; Molath, A.; Choksi, H.; Kumar, S.; Mehra, R. Classifications of Polyphenols and Their Potential Application in Human Health and Diseases. *Int. J. Physiol. Nutr. Phys. Educ.* **2021**, *6*, 293–301. [CrossRef]
16. Samanta, S.; Sarkar, T.; Chakraborty, R.; Rebezov, M.; Shariati, M.A.; Thiruvengadam, M.; Rengasamy, K.R. Dark Chocolate: An Overview of Its Biological Activity, Processing, and Fortification Approaches. *Curr. Res. Food Sci.* **2022**, *5*, 1916–1943. [CrossRef]
17. Hano, C.; Tungmunnithum, D. Plant Polyphenols, More than Just Simple Natural Antioxidants: Oxidative Stress, Aging and Age-Related Diseases. *Medicines* **2020**, *7*, 26. [CrossRef]
18. Di Lorenzo, C.; Colombo, F.; Biella, S.; Stockley, C.; Restani, P. Polyphenols and Human Health: The Role of Bioavailability. *Nutrients* **2021**, *13*, 273. [CrossRef]
19. Mustafa, Y.F.; Bashir, M.K.; Oglah, M.K. Original and Innovative Advances in the Synthetic Schemes of Coumarin-Based Derivatives: A Review. *Syst. Rev. Pharm.* **2020**, *11*, 598–612.
20. Khursheed, A.; Jain, V. Medicinal Research Progress of Natural Coumarin and Its Derivatives. *Nat. Prod. J.* **2021**, *11*, 648–662. [CrossRef]
21. Li, H.; Li, M.; Xu, R.; Wang, S.; Zhang, Y.; Zhang, L.; Zhou, D.; Xiao, S. Synthesis, Structure Activity Relationship and in Vitro Anti-Influenza Virus Activity of Novel Polyphenol-Pentacyclic Triterpene Conjugates. *Eur. J. Med. Chem.* **2019**, *163*, 560–568. [CrossRef]
22. Vega-Granados, K.; Medina-O'Donnell, M.; Rivas, F.; Reyes-Zurita, F.J.; Martinez, A.; Alvarez De Cienfuegos, L.; Lupiañez, J.A.; Parra, A. Synthesis and Biological Activity of Triterpene–Coumarin Conjugates. *J. Nat. Prod.* **2021**, *84*, 1587–1597. [CrossRef] [PubMed]
23. Yarden, Y.; Pines, G. The ERBB network: At last, cancer therapy meets systems biology. *Nat. Rev. Cancer* **2012**, *12*, 553–563. [CrossRef] [PubMed]
24. Normanno, N.; De Luca, A.; Bianco, C.; Strizzi, L.; Mancino, M.; Maiello, M.R.; Carotenuto, A.; De Feo, G.; Caponigro, F.; Salomon, D.S. Epidermal growth factor receptor (EGFR) signalling in cancer. *Gene* **2006**, *366*, 2–16. [CrossRef] [PubMed]
25. Mustafi, R.; Dougherty, U.; Shah, H.; Dehghan, H.; Gliksberg, A.; Wu, J.; Zhu, H.; Joseph, L.; Hart, J.; Dive, C.; et al. Both stromal cell and colonocyte epidermal growth factor receptors control HCT116 colon cancer cell growth in tumor xenografts. *Carcinogenesis* **2012**, *33*, 1930–1939. [CrossRef]
26. Geißler, A.L.; Geißler, M.; Kottmann, D.; Lutz, L.; Fichter, C.D.; Fritsch, R.; Weddeling, B.; Makowiec, F.; Werner, M.; Lassmann, S. ATM mutations and E-cadherin expression define sensitivity to EGFR-targeted therapy in colorectal cancer. *Oncotarget* **2017**, *8*, 17164–17190. [CrossRef]
27. Mac, L. Egfr in the hct-116 line of human colorectal cancer cells. *Adv. Cell Sci. Tissue Cult.* **2022**, *6*, 122.
28. Ayadi, J.; Debouba, M.; Rahmani, R.; Bouajila, J. The Phytochemical Screening and Biological Properties of *Brassica napus* L. Var. *Napobrassica* (Rutabaga) Seeds. *Molecules* **2023**, *28*, 6250. [CrossRef]
29. Ben Khadher, T.; Sassi-Aydi, S.; Aydi, S.; Mars, M.; Bouajila, J. Phytochemical Profiling and Biological Potential of Prunus Dulcis Shell Extracts. *Plants* **2023**, *12*, 2733. [CrossRef]
30. Trott, O.; Olson, A.J. AutoDock Vina: Improving the Speed and Accuracy of Docking with a New Scoring Function, Efficient Optimization, and Multithreading. *J. Comput. Chem.* **2010**, *31*, 455–461. [CrossRef]
31. Vardanega, R.; Santos, D.T.; Meireles, M.A.A. Intensification of Bioactive Compounds Extraction from Medicinal Plants Using Ultrasonic Irradiation. *Pharmacogn. Rev.* **2014**, *8*, 88. [CrossRef] [PubMed]
32. Gadjalova, A.V.; Mihaylova, D. Ultrasound-Assisted Extraction of Medicinal Plants and Evaluation of Their Biological Activity. *Food Res.* **2019**, *3*, 530–536. [CrossRef]
33. Xie, P.; Huang, L.; Zhang, C.; Deng, Y.; Wang, X.; Cheng, J. Enhanced Extraction of Hydroxytyrosol, Maslinic Acid and Oleanolic Acid from Olive Pomace: Process Parameters, Kinetics and Thermodynamics, and Greenness Assessment. *Food Chem.* **2019**, *276*, 662–674. [CrossRef]
34. Yang, K.; Wang, S.-B.; Pei, D.; Pu, L.-M.; Huang, X.-Y. Effective Separation of Maslinic Acid and Oleanolic Acid from Olive Pomace Using High-Speed Shear off-Line Coupled with High-Speed Countercurrent Chromatography and Their Antibacterial Activity Test. *J. Chromatogr. B* **2024**, *1236*, 124069. [CrossRef] [PubMed]

35. Cheng, K.; Su, C.; Huang, J.; Liu, J.; Zheng, Y.; Chen, Z. Conjugation of Uridine with Oleanolic Acid Derivatives as Potential Antitumor Agents. *Chem. Biol. Drug Des.* **2016**, *88*, 329–340. [CrossRef] [PubMed]
36. Chen, L.; Zhu, Z.F.; Meng, F.; Xu, C.S.; Zhang, Y.H. Synthesis and Cytotoxicity of Oleanolic Acid/N-Aryl-N′-Hydroxyguanidine Hybrids. *Chin. J. Nat. Med.* **2010**, *8*, 436–440. [CrossRef]
37. Bednarczyk-Cwynar, B.; Günther, A. Advances in Chemistry and Pharmacology of Triterpenoid Synthetic Dimers. *Curr. Med. Chem.* **2017**, *24*, 2205–2240. [CrossRef]
38. Zhang, X.; Zheng, Y.-Y.; Hu, C.-M.; Wu, X.-Z.; Lin, J.; Xiong, Z.; Zhang, K.; Xu, X.-T. Synthesis and Biological Evaluation of Coumarin Derivatives Containing Oxime Ester as α-Glucosidase Inhibitors. *Arab. J. Chem.* **2022**, *15*, 104072. [CrossRef]
39. Xu, X.-T.; Deng, X.-Y.; Chen, J.; Liang, Q.-M.; Zhang, K.; Li, D.-L.; Wu, P.-P.; Zheng, X.; Zhou, R.-P.; Jiang, Z.-Y. Synthesis and Biological Evaluation of Coumarin Derivatives as α-Glucosidase Inhibitors. *Eur. J. Med. Chem.* **2020**, *189*, 112013. [CrossRef]
40. Günther, A.; Zalewski, P.; Sip, S.; Ruszkowski, P.; Bednarczyk-Cwynar, B. Acetylation of Oleanolic Acid Dimers as a Method of Synthesis of Powerful Cytotoxic Agents. *Molecules* **2024**, *29*, 4291. [CrossRef]
41. Günther, A.; Zalewski, P.; Sip, S.; Ruszkowski, P.; Bednarczyk-Cwynar, B. Oleanolic Acid Dimers with Potential Application in Medicine—Design, Synthesis, Physico-Chemical Characteristics, Cytotoxic and Antioxidant Activity. *Int. J. Mol. Sci.* **2024**, *25*, 6989. [CrossRef] [PubMed]
42. Karjalainen, A.; Doan, P.; Chandraseelan, J.G.; Sandberg, O.; Yli-Harja, O.; Candeias, N.R.; Kandhavelu, M. Synthesis of Phenol-Derivatives and Biological Screening for Anticancer Activity. *AntiCancer Agents Med. Chem.* **2017**, *17*, 1710–1720. [CrossRef]
43. Annunziata, F.; Pinna, C.; Dallavalle, S.; Tamborini, L.; Pinto, A. An Overview of Coumarin as a Versatile and Readily Accessible Scaffold with Broad-Ranging Biological Activities. *Int. J. Mol. Sci.* **2020**, *21*, 4618. [CrossRef] [PubMed]
44. Phutdhawong, W.; Chuenchid, A.; Taechowisan, T.; Sirirak, J.; Phutdhawong, W.S. Synthesis and Biological Activity Evaluation of Coumarin-3-Carboxamide Derivatives. *Molecules* **2021**, *26*, 1653. [CrossRef]
45. Martínez-Lara, R.I.; Cobos-Ontiveros, L.A.; Meza-Ireta, S.A.; Martínez-Montiel, M.; Colín-Lozano, B.; Puerta, A.; Padrón, J.M.; López, Ó.; Vega-Báez, J.L.; Merino-Montiel, P.; et al. Novel Coumarin-steroid/Terpenoid Hybrids: In Vitro and in Silico Anticancer Studies. *Chem. Biodivers.* **2024**, *21*, e202401315. [CrossRef] [PubMed]
46. Herrera-R, A.; Naranjo, T.W.; Maldonado, M.E.; Moreno-Q, G.; Yepes, A.; Cardona-G, W. Styrylcoumarin 7-SC2 Induces Apoptosis in SW480 Human Colon Adenocarcinoma Cells and Inhibits Azoxymethane-Induced Aberrant Crypt Foci Formation in BALB/c Mice. *Med. Chem. Res.* **2020**, *29*, 377–395. [CrossRef]
47. Holbro, T.; Hynes, N.E. ErbB Receptors: Directing Key Signaling Networks Throughout Life. *Annu. Rev. Pharmacol. Toxicol.* **2004**, *44*, 195–217. [CrossRef]
48. Guérin, O.; Fischel, J.L.; Ferrero, J.-M.; Bozec, A.; Milano, G. EGFR Targeting in Hormone-Refractory Prostate Cancer: Current Appraisal and Prospects for Treatment. *Pharmaceuticals* **2010**, *3*, 2238–2247. [CrossRef]
49. Abdelgawad, M.A.; Bakr, R.B.; Alkhoja, O.A.; Mohamed, W.R. Design, Synthesis and Antitumor Activity of Novel Pyrazolo [3, 4-d] Pyrimidine Derivatives as EGFR-TK Inhibitors. *Bioorganic Chem.* **2016**, *66*, 88–96. [CrossRef]
50. Maennling, A.E.; Tur, M.K.; Niebert, M.; Klockenbring, T.; Zeppernick, F.; Gattenlöhner, S.; Meinhold-Heerlein, I.; Hussain, A.F. Molecular Targeting Therapy against EGFR Family in Breast Cancer: Progress and Future Potentials. *Cancers* **2019**, *11*, 1826. [CrossRef]

Disclaimer/Publisher's Note: The statements, opinions and data contained in all publications are solely those of the individual author(s) and contributor(s) and not of MDPI and/or the editor(s). MDPI and/or the editor(s) disclaim responsibility for any injury to people or property resulting from any ideas, methods, instructions or products referred to in the content.